2020년 2월

석사학위논문

다양한 나노fiber를 활용한 효소의 고정화 및 재사용

조선대학교 대학원

화 학 공 학 과

오 소 걸

다양한 나노fiber를 활용한 효소의 고정화 및 재사용

Immobilization of Organophosphorus Hydrolase, Lysine Decarboxylase, Glutamate Decarboxylase and ω-Transaminases onto Various Polymer Nanofibers for Enzyme Stabilization and Recycling

2020년 2월 25일

조선대학교 대학원

화 학 공 학 과

오 소 걸

다양한 나노fiber를 활용한 효소의 고정화 및 재사용

지도교수 이 중 헌

이 논문을 공학 석사학위신청 논문으로 제출함

2019년 10월

조선대학교 대학원

화 학 공 학 과

오 소 걸

오소걸의 석사학위논문을 인준함

위원장 조선대학교 교수 이 재 욱 (인)

위 원 조선대학교 교수 신 현 재 (인)

위 원 조선대학교 교수 이 중 헌 (인)

2019년 11월

조선대학교 대학원

Contents

List of Figures

List of Tables

ABSTRACT

Immobilization of Organophosphorus Hydrolase, Lysine Decarboxylase, Glutamate Decarboxylase and ω-Transaminases onto Various Polymer Nanofibers for Enzyme Stabilization and Recycling

Wu Xiaojie

Advisor : Prof. Jung-Heon Lee, Ph.D.

Department of Chemical Engineering

Graduate School of Chosun University

Enzymes are often hampered by their reuse and cumbersome recovery and by lack of their long-term operational stability. These drawbacks can be overcome by immobilization of enzymes. Therefore, four different polymer nanofibers, foam-polyaniline nanofiber (foam-PANI), foam-magnetically separable polyaniline nanofiber (foam-PAMP), foam-polydopamine nanospheres (foam-PDA), and foam-tannic acid & $FeCl_3$ (foam-TA) have been used for the surface coating of nickel foams and they have used for the immobilization of organophosphorus hydrolase (OPH), lysine decarboxylase (LDC), glutamate decarboxylase (GAD) and ω-transaminases (ω-TA). These four polymers have shown excellent properties.

1. Immobilization of OPH onto nickel foam coated with PANI, PAMP, PDA, and TA in the following ways: by cross-linking randomly OPH to polymer nanofibers-coated nickel foam using glutaraldehyde. After 70 cycles reuse of foam-PANI-, foam-PAMP-, foam-PDA-, and foam-TA-OPH under relevant process conditions, they showed high stability and maintained high conversion (70 %, 72 %, 63 %, and 78 %). The relative activities of foam-PANI-, foam-PAMP-,

foam-PDA-, and foam-TA-OPH were 87 %, 79 %, 62 %, and 83 % of the initial activity retained, respectively after 3 months of vigorous shaking conditions at room temperature (25℃). The OPH immobilization onto four polymer nanofibers provides a practical method for the detoxification of organophosphate pesticides.

2. Cadaverine was produced by decarboxylation of lysine using LDC. Foam-PANI, foam-PAMP, foam-PDA, and foam-TA have been used as LDC immobilization carriers for stabilization and recycle. The free LDC lost 40 % of the its initial activity after 3 months under vigorous shaking conditions at room temperature, but the immobilized LDCs on foam-PANI, foam-PAMP, foam-PDA, and foam-TA lost only 0 to 6 % their initial activity. The immobilized LDCs with foam-PANI, foam-PAMP, foam-PDA, and foam-TA showed a high percentage of conversion (83 %, 80 %, 64 %, and 75 %) after 80 reaction cycles reuse.

3. The immobilized GADs on foam-PANI, foam-PAMP, foam-PDA, and foam-TA have been used for the production of gamma-aminobutyric acid (GABA) from glutamate. The immobilization yields after immobilization onto four different carriers, foam-PANI, foam-PAMP, foam-PDA, and foam-TA were 67 %, 70 %, 69 %, and 74 %, respectively. 62 %, 58 %, 47 %, and 54 % of monosodium glutamate (MSG) were converted to GABA after 48 h reaction. The immobilized GADs retained 89 %, 88 %, 42 %, and 81 % of their initial activities after 3 months of vigorous shaking conditions at room temperature.

4. ω-TA is one of important biocatalyst and is widely used for the production of chiral amines. The immobilized ω-TAs on foam-PANI, foam-PAMP, foam-PDA, and foam-TA were prepared and used to enhance the stability and recyclability. The immobilized ω-TAs on foam-PANI, foam-PAMP, foam-PDA, and foam-TA retained 42 %, 28 %, 22 %, and 41 % of their initial conversion after 10 cycles. Immobilized ω-TAs on foam-PANI- and foam-TA-(ω-TA) showed 97 % and 85 % relative activity, respectively.

Ⅰ. Development of enzyme immobilization carrier

1. Introduction

a. Background of enzyme immobilization

Applications of enzymes in different industries are continuously increasing. Researchers are finding their applications in food, textiles, pulp and paper, and detergents industries. Moreover, the use of enzymes has become an inevitable processing strategy in healthcare and pharmaceutical sectors. However, enzymes are generally expensive, and are also highly sensitive to various denaturing conditions when isolated from their natural environments. Their sensitivity can act as inhibitors which add to their costs. Additionally, enzymes are often hampered by their reuse and cumbersome recovery and by lack of their long-term operational stability. These drawbacks can be overcome by immobilization of enzymes.

Immobilization is a technical process in which enzymes are fixed within solid supports, such as calcium alginate or silica, creating a heterogeneous immobilized enzyme system. The solid support systems, generally stabilize the structure and activities of the enzymes. As a consequence, compared to free enzymes in solution, the immobilized enzymes are more resistant and more robust to environmental changes, allow the easy recovery of both products and enzymes, rapid termination of reactions, continuous operation of enzymatic processes, multiple reuse of enzymes, and greater variety of bioreactor designs [1].

Generally, four methods are used for enzyme immobilization, namely (a) non-covalent adsorption and deposition, (b) physical entrapment, (c) covalent attachment, and (d) bio-conjugation (Figure 1) [2].

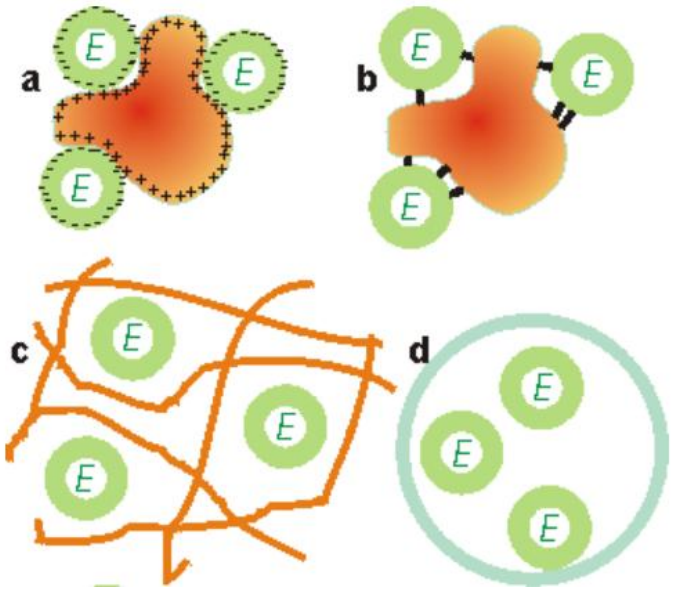

Figure 1. Enzyme immobilization systems (a) carrier-bound enzyme; (b) cross-linked enzyme; (c) enzyme inclusion; (d) microcapsule [2].

In short, enzymes can be immobilized by various means, however, in order to provide weak physical interaction or strong chemical bonding, water-insoluble materials must be used as a fixed carrier. However, any immobilization methods or carriers cannot be applied to all enzymes. In order to achieve better immobilization effect, it is necessary to select suitable immobilization methods and carriers according to specific enzymes and catalytic reaction types. In consideration of high load rate, intensity, and specific surface area, nanomaterials have been considered as the promising carriers for enzyme immobilization [3]. In the present work, four different polymer nanofibers, namely, PANI, PAMP, PDA, and TA have been used for the immobilization of enzymes. In order to improve the recovery of immobilized enzymes more easily, the author used nickel foam (Figure 2) with unique pore structure, inherent tensile strength and thermal shock resistance to graft four polymer nanofibers by physical methods, making the new four carriers, that is, foam-PANI, foam-PAMP, foam-PDA and foam-TA.

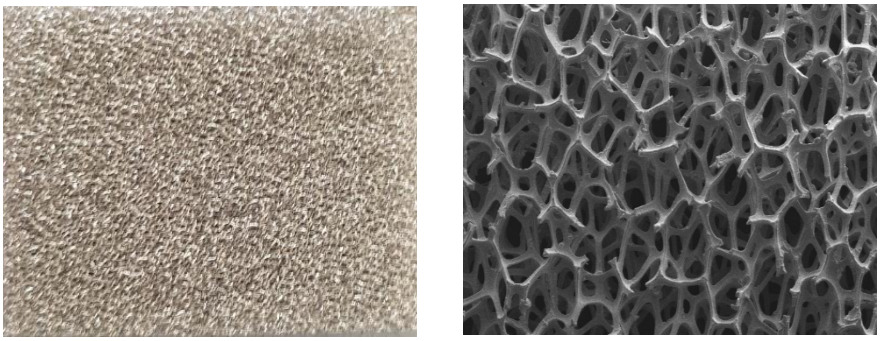

Figure 2. SEM images of nickel foam.

b. New immobilization carriers

(1) Polyaniline nanofibers (PANI)

Polyaniline is one of the most widely used conducting polymer for many applications since it possesses novel properties such as semi-conductivity, electrical activity and excellent environment stability [4, 5]. The nanostructured polyanilines can enhance diffusion rates and biomolecule interactions by providing highly hydrophilic and porous structures with smaller fiber diameters. Recently, nanostructured polyanilines have been incorporated with different transducers and actuators for the sensing and detections of DNA, drugs and enzymes [6]. PANI was successfully synthesized by rapid mixing polymerization method using ammonium persulfate as an initiator and the aniline as a monomer in 1M HCl (Figure 3). The composite form of PANI has been used in a number of applications, including in anti-corrosive coatings, energy storage and conversion systems, gas sensors, and electrocatalytic devices. Additionally, PANI has also been widely exploited as a potential material for tunable electrical, biosensing and optical properties [7, 8]. This study explores the applications and advantages of enzymes immobilization onto polyaniline nanofibers grafted nickel foam and the remaining challenges in developing better products.

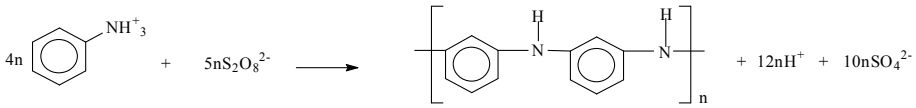

Figure 3. PANI synthesis with APS as oxidant.

(2) Magnetically separable polyaniline nanofibers (PAMP)

Functionalized magnetic nanomaterials are found as a practically useful support for enzyme immobilization due to readily recyclability [3, 9]. Some studies have been reported that immobilization of enzymes onto magnetic nanomaterials. Lipase, laccase, and cholesterol oxidase, etc. have been immobilized onto different magnetic nanomaterials and exhibited good reusability and stability [3].

PAMP is synthesized by adding Fe_3O_4 in the process of synthesizing polyaniline [10]. PAMP were synthesized using a mixture of iron oxide and nanofibers and the aniline solution. PAMP can be separated from the reaction mixture by using magnet [11]. Magnetic polymer materials have special properties due to their low density, good processability, film formation, the introduction of specific functional groups, and excellent properties not found in conventional inorganic magnetic materials, which can meet the special needs of many materials. Therefore, its application prospects are very broad. Literature studies have shown that there is an interaction between polyaniline chains and metal ions to produce conductive polymer complexes with excellent physical and chemical properties. When a conductive polymer reacts with a metal ion, it is actually a metal ion that interacts with a nitrogen atom on the conductive polymer chain (Figure 4) [12].

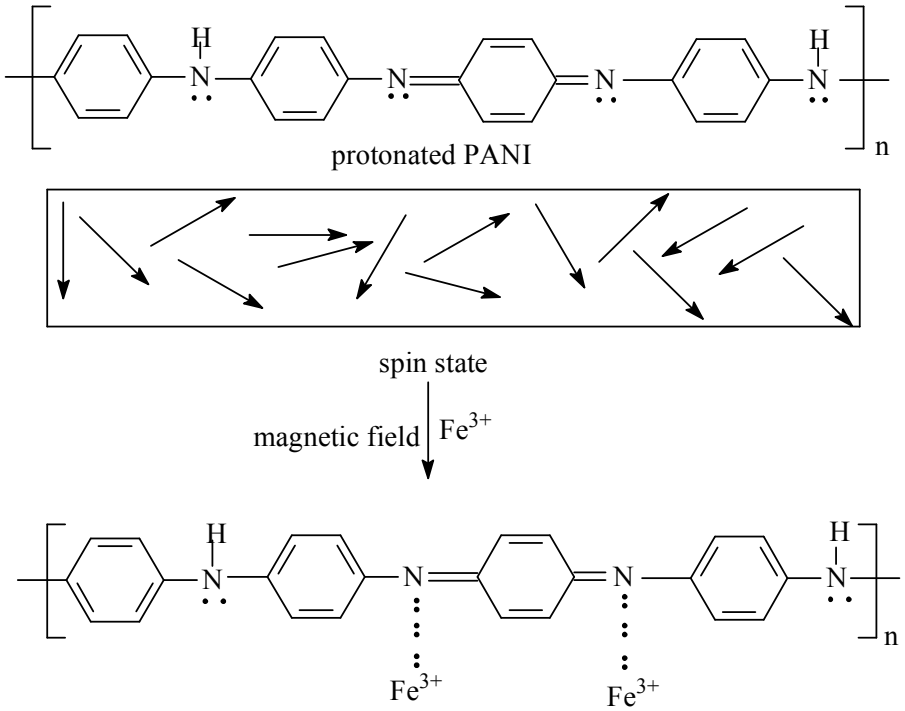

Figure 4. Schematic diagram of the ferromagnetic conductive PANI-$Fe3^{+}$ formation mechanism under magnetic field [12].

(3) Polydopamine (PDA) nanospheres

Since the scientists have discovered that the dopamine (DA) molecules can imitate mussel adhesive proteins to self-aggregate in an alkaline aerobic water environment, the mechanism involved in the formation process has not been fully understood. However, due to potential applications in the field of surface modification, DA is still a hot topic of interest. DA has been widely used in biomaterials surface modification for possible further addition reactions with mercapto groups or amino groups. Moreover, the film surface could be fixed by biologically active molecules such as proteins, growth factors, polysaccharides [13].

At present, most researchers infer that the process of dopamine self-polymerization is similar to the process of melanin production in organisms (Figure 5). Dopamine self-polymerizes to form PDA in an oxidizing agent under a weakly alkaline environment. PDA can be deposited on various materials' surface including polymers, metal oxides, metals, and even on super-hydrophobic materials without limiting the three-dimensional structure. PDA coating shows great potential by providing advantages, such as multifunctional groups, versatile adhesive properties for inorganic and organic substrates, nanostructures, hydrophilic and non-toxic properties, self-reducing ability, and in situ N-doping through carbonization for enhancing catalytic performance [14, 15]. This indicates a huge potential for various applications.

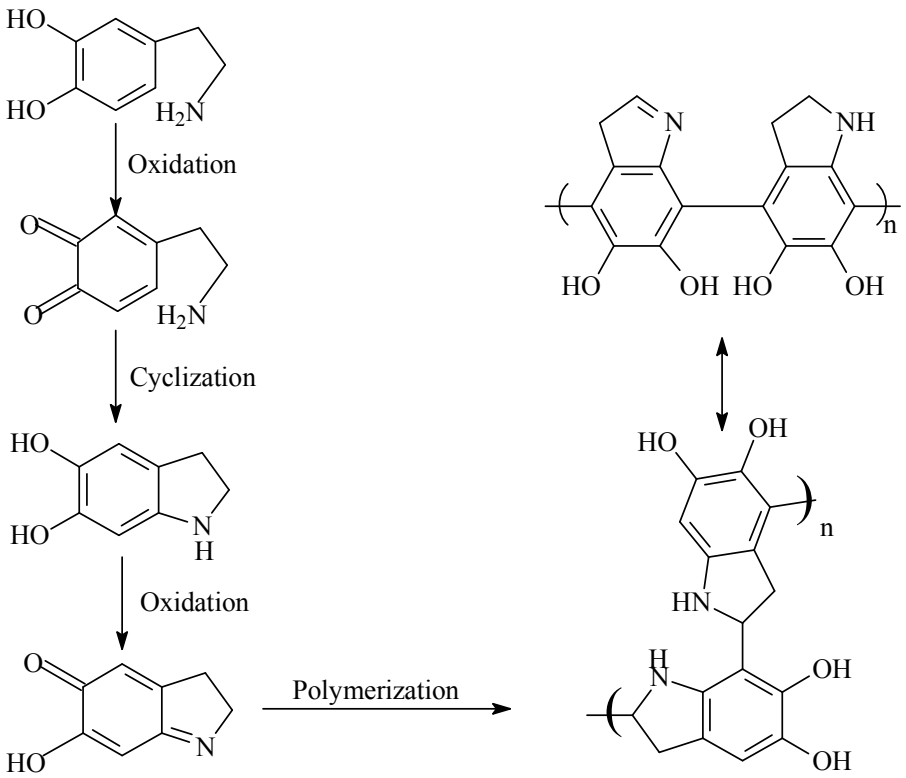

Figure 5. Schematic diagram of dopamine self-polymerization [13].

(4) Metal polyphenol complexes (tannic acid&$FeCl_3$)

Tannic acid (TA) is one of the plant polyphenolic compounds which can be widely found in plant roots, stems, leaves and fruits [16]. Polyphenolic compounds contain phenolic hydroxyl groups, which can be polymerized by covalent bonds or hydrogen bonds [17]. Metal chelates made by condensing Fe^{3+} ions and natural polyphenol tannins from aqueous solution can coat flat surfaces and change surface morphology. Three galloyl groups from TA can react with each Fe^{3+} ion to form a stable octahedral complex, allowing each TA molecule to react with several Fe^{3+} centers to form a cross-linked film (Figure 6a). Studies have shown that an excess of ferric ions can form capsule particles, and within a certain range, the higher the iron ion content, the thicker the film is formed [18]. The binding reaction between plant polyphenols and proteins is the most important chemical characteristic, and the intensive research work has been carried out in this field. The "glove-hand" reaction model (Figure 6b) proposed by Haslam et al. in the 1980s is now most widely accepted. The main reaction mechanism is that plant polyphenols first approach the surface of protein molecules through hydrophobic bonds, and polyphenols enter the hydrophobic bag, then multi-point hydrogen bonding occurs. The complex reactions of plant polyphenols with alkaloids, polysaccharides, nucleic acids, cell membranes and other biological macromolecules are similar [19].

(a)

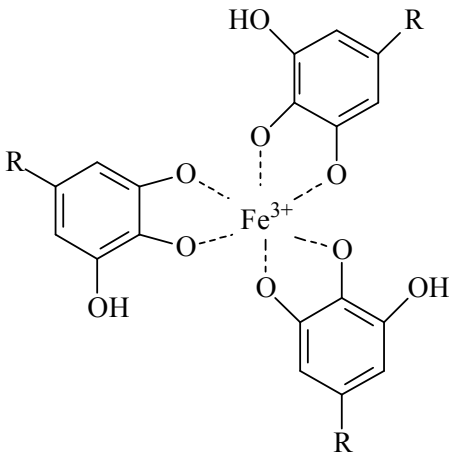

(b)

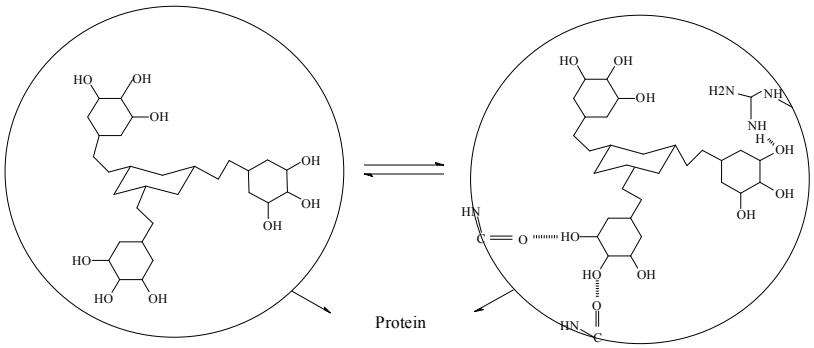

Figure 6. (a) The molecular structure of TA＆FeCl3·6H2O; (b) schematic diagram of protein reaction with plant polyphenols.

2. Materials

The aniline, DA, TA, ammonium persulfate (APS) and $FeCl_3$ used in the synthesis of four different polymer nanomaterials were purchased from Sigma-Aldrich (St. Louis. USA). Hydrochloric acid (HCl) was supplied by Daejung (Korea).

3. Method for preparing immobilization carrier

a. Preparation of foam-PANI and foam-PAMP

Foam-PANI and foam-PAMP were prepared by using the method developed by Lee et al. [20]. Polyaniline nanofibers were synthesized from rapidly mixed reactions. First, 0.1 M of an initiator (APS), 10 nickel foam and 7.5 wt% of an aniline monomer solution in 1 M hydrochloric acid were mixed rapidly and were shaken nearly 18 h at 200 rpm. Addition of 10 % (w/v) of iron oxide nanoparticles to the polyaniline mixture rendered the polyaniline magnetically nanofiber. Once the initiator molecules had been depleted during nanofiber formation, there was no further polymerization that could lead to overgrowth. The nickel foam was washed with distilled water (pH 3.5) to remove the remaining hydrochloric acid and was stored in a refrigerator for further use.

b. Preparation of foam-PDA

Foam-PDA was prepared by using the method developed by Jiang et al. [21]. The foam-PDA was directly polymerized in a water-alcohol mixed solution of a weakly basic mixed solvent system at room temperature. Firstly, ethanol solution 40 mL of 30 wt% was prepared followed by addition of 10 Ni-foam and 200 μL of weak alkali ammonia water which can affect the size of the PDA sphere to the ethanol solution. The mixture was gently stirred for 30 min at room temperature. Lastly, 0.5 g of dopamine hydrochloride (with different weight fractions) was added directly to the mixed solution. The color of the solution changed from light brown to dark brown immediately within 24 h of gentle shaking. The samples were washed with distilled water until there were no more color falling.

c. Preparation of foam-TA

Foam-TA was prepared by using the method developed by Zhang et al. [22]. The TA molecule chelates iron ions to form a coordination complex, and the resulting crosslinked polymer was physically deposited on the surface of the Ni-foam. Firstly, the solution (4 % w/v) of TA with different weight fractions was prepared. After that, the 10 Ni-foam was added under room temperature at 200 rpm for 30 min followed by 0.75 % (w/v) $FeCl_3$ (with different weight fractions) was added directly to the solution. This mixture was allowed to fully react under room temperature at 200 rpm for 40 h. The samples were washed with distilled water until there were no more color falling.

4. Results and discussion

The FTIR spectrum provides direct evidence for the synthesis of various polymeric materials.

a. The FTIR spectrum of PANI was shown in Figure 7a. The absorption peaks at 1578 cm^{-1} and 1489 cm^{-1} were attributed to the C=C stretching of the quinoid and the benzene rings, indicating the oxidation state of emeraldine salt of PANI. The peak at 1292 cm^{-1} and 1240 cm^{-1} were attributed to the bending vibration of C-N to aromatic amine/imine and the stretching vibration of C-N in polarized structure. And the peak at 1128 cm^{-1} explained the aromatic C-H in-plane bending vibration, which is often related to the doped structure. The observed bands at 878 cm^{-1}, 769 cm^{-1} and 690 cm^{-1} can be assigned to the aromatic ring, the out-of-plane deformation vibration of the C-H bond in the benzene ring and the distributed aromatic ring indicating the formation of the polymer [23-27].

b. The peak shape of PAMP was roughly equivalent (Figure 7b). However, PAMP has the participation of Fe_3O_4, the peak shifting could be due to bond formation between Fe_3O_4 and polyaniline at 1296 cm^{-1} and 1242 cm^{-1}.

c. The FTIR spectrum of PDA was shown in Figure 7c. The peak appears at 3500-3000 cm^{-1} in the spectrum, which was attributed to the stretching vibration of N-H and O-H, and the vibration peaks at 1558 and 1506 cm^{-1} belongs to stretching of indole aromatic C=C bonds and C=N bonds, the vibration peak at 1282 cm^{-1} was associated with the tensile vibration of C-O-H on the benzene rings, and at 1118 cm^{-1} respectively belongs to the shear vibration of C-O [28, 29].

d. The FTIR spectra of TA&$FeCl_3 \cdot 6H_2O$ complex was shown in Figure 7d. The broadband in the range of 3500-3000 cm^{-1} was hydrogen bond -OH tensile vibration and the peak at 1704 cm^{-1} was attributed to the C=C bond on the benzene ring. Due to the C-C tensile vibration and C-H bond on the benzene ring, the stretching of the C-O band, the peaks at 1083 and 1022 cm^{-1} belong to O-H of phenolic [30-32].

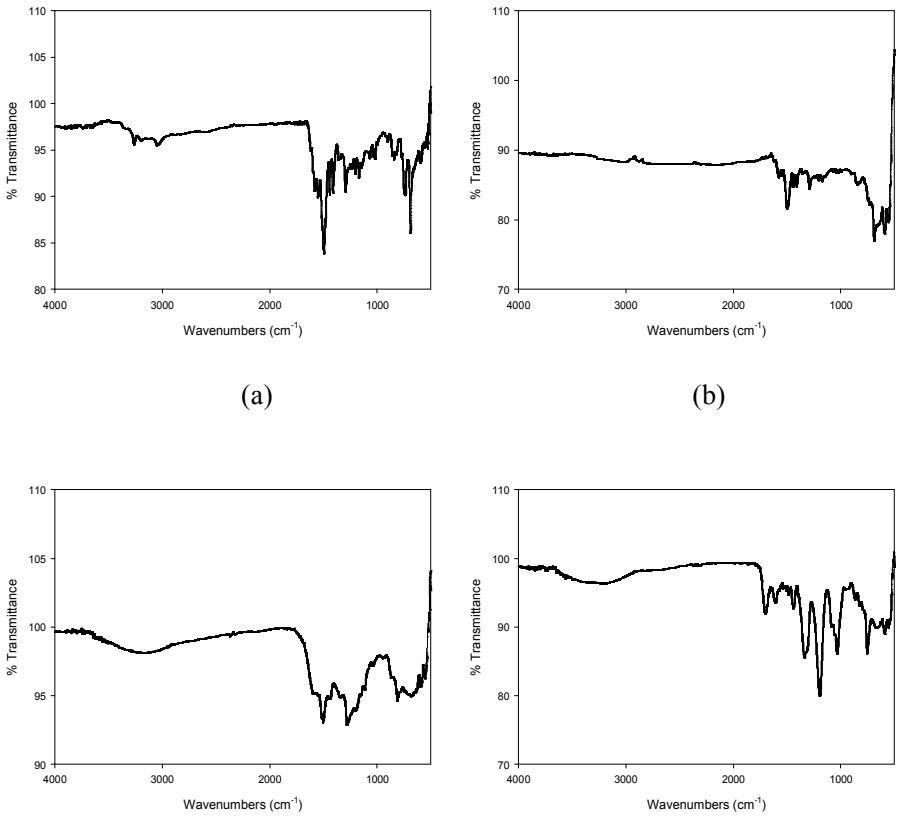

Figure 7. FTIR spectra of nickel foam after (a) PANI; (b) PAMP; (c) PDA; (d) TA coating.

Ⅱ. Immobilization of enzymes onto various polymer nanofibers for enzyme stabilization

A. Immobilization of OPH onto various polymer nanofibers for enzyme stabilization

1. Introduction

OPH, also known as phosphotriesterase, hydrolyzes a broad range of organophosphates, such as certain pesticides and nerve gas agents [33]. This enzyme catalyzes the hydrolysis of the phosphoester bond in orthophosphates (Figure 8).

The organophosphate pesticides, though very important for the growth of the agricultural industry, have some adverse effects on the environment. Notable published concerns have indicated that some proportion of pesticides residues in food products and contaminates the water supplies [34]. It is estimated that up to 800,000 individuals each year are affected by pesticide poisoning, therefore, the current environmental problems associated with contamination and pesticide usage require serious attention [35]. Recently, the utilization of OPH in sensors which are being used in the degradation of hazardous organophosphates and these toxic compounds, has received researcher's attention [34, 36, 37]. For example, OPH-based sensors and assays have been used to determine pesticide concentration. Caldwell and Raushel demonstrated the detoxification of organophosphate pesticides through OPH immobilization [33].

In the present research, the OPH was covalently immobilized onto the four different polymer nanofibers, and the capability of immobilized OPH to catalyze the hydrolysis of organophosphate pesticides was described.

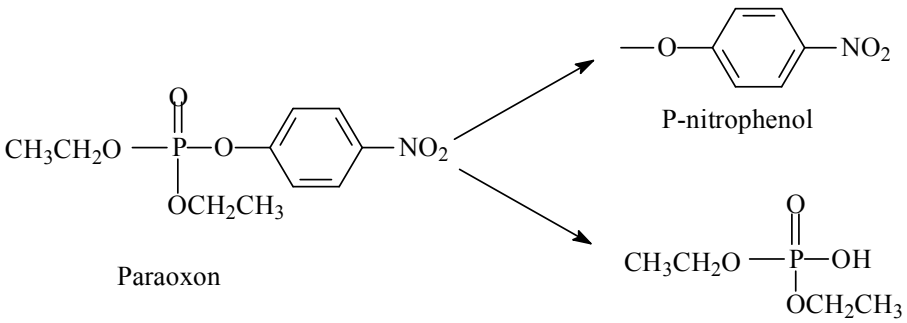

Figure 8. Biodegradation of paraoxon to *p*-nitrophenol using OPH.

2. Materials

Yeast extract, KH_2PO_4, H_2SO_4, $MgSO_4$, $CaCl_2$, $CoCl_2$, $FeSO_4$, $Na_2HPO_4 \cdot 7H_2O$ were obtained from Fisher Scientific. Anti-foam, paraoxon, *p*-nitrophenol, CHES, glutaraldehyde solution (GA), tris (hydroxymethyl) aminomethane were purchased from Sigma-Aldrich. NH_4Cl, NaCl, tryptone, agar, isopropyl-beta-D-thiogalactopyranoside (IPTG), glycerol were supplied by Baker.

Instruments such as sonic dismemberator (Fisher 100 model), fermenter (Biotron Co. Korea), and incubator (HANBAEK ST CO. Korea), small high speed refrigerated centrifuge (Hanil, Korea), autoclave (HANBAEK ST CO. Korea), deep freezer (DF8517, Il-Shin Bio Co.) were used.

3. Strain and storage

The strain was a recombinant *Escherichia coli* producing OPH. Cells were grown at 37 , 200 rpm until the OD_{600} reached 0.6 ~ 0.8. 50 % glycerol was added at a ratio of 1:1 (v/v) and mixed completely. Store in a deep freezer at -70 for further use.

4. Medium composition

The LB medium for activation consisted of tryptone, NaCl, and yeast extract. The fermentation medium was composed of yeast extract, glucose, NH_4Cl, NaCl, KH_2PO_4, Na_2HPO_4, and trace elements $CaCl_2$, $CoCl_2$, $MgSO_4$ (Table 1).

Table 1. Media composition for recombinant *Escherichia coli* culture for the production of OPH

Component	Concentration	Medium type
Tryptone	1 g/L	LB medium
NaCl	1 g/L	
Yeast extract	0.5 g/L	
Glucose	40 g/L	Fermentation medium
KH_2PO_4	3 g/L	
NaCl	0.5 g/L	
NH_4Cl	1 g/L	
Na_2HPO_4	6.78 g/L	
Yeast Extract	2 g/L	
$MgSO_4$	1 mM/L	
$CaCl_2$	0.5 mM/L	
$CoCl_2$	0.5 mM/L	

5. Production of OPH

a. Culture conditions

A fresh colony from the overnight LB agar plate was inoculated on the LB medium and the cells were grown overnight in a shake flask (37℃, at 200 rpm). The seed culture (100 mL) was inoculated into a 2 L fermenter and cultured at 37℃, 200 rpm until the OD_{600} reached 5 (Exponential growth period). For induction, IPTG (24 mg/mL) was added and the culture was shaken for further 16 h at 16℃， 200 rpm.

b. Enzyme activity assays of OPH

(1). Preparation of cell extracts

The cells were harvested by centrifugation (3,000×*g*, 4℃, and 20 min) and concentrated 50 times with 500 mM sodium phosphate buffer (pH 6.5). Cell extracts were prepared by twenty sonications (2 s each) of washed cell suspensions (2 mL of 500 mM sodium phosphate buffer, pH 6.5) with cooling intervals of 3 s. Cell debris was removed by centrifugation.

(2). Analytical methods

The activities of the free and immobilized OPHs were determined at room temperature using chromogen paraxon as the substrate. The reaction mixture contained 125 mM CHES buffer (pH 9.0), and 10 mM paraxon. After adding the free or immobilized OPH, the absorbance was detected at 400 nm with a spectrophotometer.

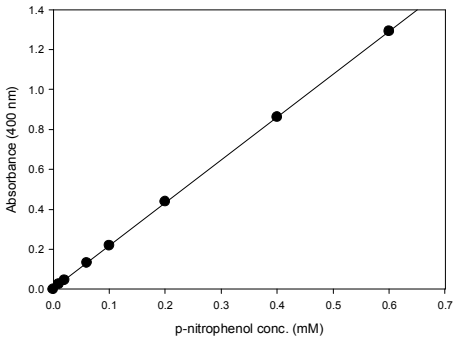

(a)

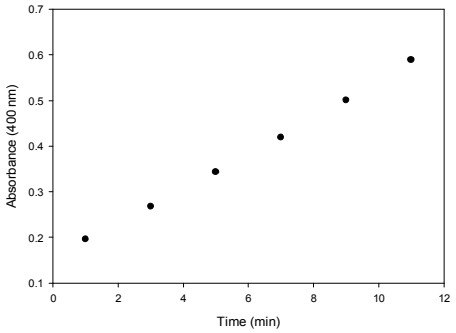

(b)

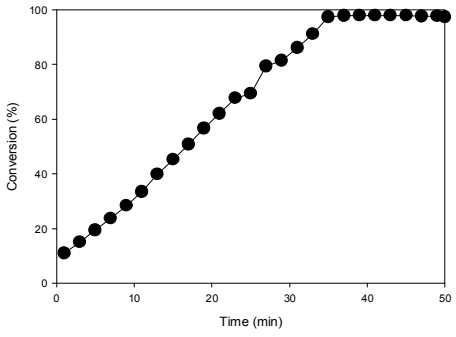

(c)

Figure 9. (a) Standard curve for the determination of *p*-nitrophenol concentration; (b) activity assay for the free OPH; (c) bioconversion with free OPH.

6. OPH immobilization

a. Protein assay

The extracted protein was quantified with the protein assay kit (Bio-Rad). First, a protein assay standard curve was obtained with Bovine serum albumin (BSA) (Figure 10).Then, 10 μL of the sample was taken and added with 90 μL of third distilled water. Next, 10 μL of diluted solution, 200 μL of protein assay kit and 790 μL of third distilled water were put in 1.5 mL tube and mixed well with a Vortex mixer and the absorbance was detected at 595 nm with a UV-spectrophotometer.

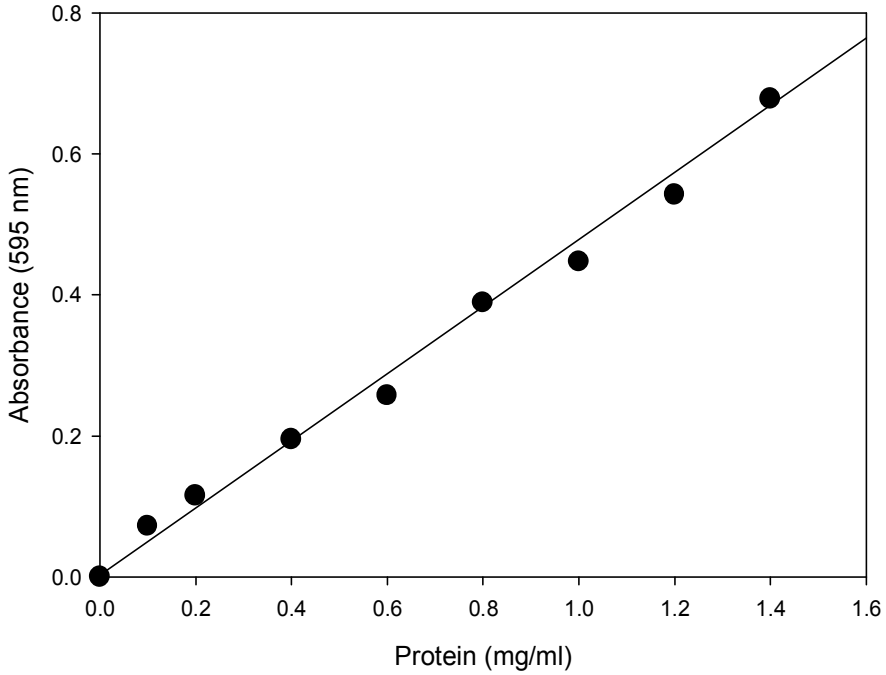

Figure 10. Standard curve of protein concentration.

b. The method of OPH immobilization

1 carrier Ni-foam and 1ml crude enzyme solution were mixed with 35 % (w/v) of ammonium sulfate in 1 mL of a 500 mM phosphate buffer (pH 6.5) and stirred gently for 30 min at room temperature. Then 1 mL of GA (1 %) as a crosslinker was added and the mixture was agitated for 17 h at 4℃, which can be enough to establish a crosslink between the enzymes. The supernatant was taken to calculate the protein concentrations, measured by the Bradford method, with the enzyme solutions before and after the GA treatment. Subsequently, 1.5 mL of 100 mM tris-HCl (pH 7.9) was added for tris-capping and shaken for 30 min to remove the remaining GA. The immobilized OPH was washed more than 10 times with a 500 mM phosphate buffer (pH 6.5) to remove the free OPHs.

In this process, the immobilization yield (IY) was calculated by using the method developed by Lee et al. [20]. The calculation equation is given below.

$$\text{IY } (\%) = \frac{E_t - E_e}{E_t} \times 100 \ \%$$

E_t: Activity of total free enzyme used

E_e: Activity of immobilized enzyme

7. Results and discussion

The free and immobilized OPHs relative activities were determined at room temperature under vigorous stirring conditions (Figure 11). The OPH immobilized onto foam-PANI, foam-PAMP and foam-TA showed above 87 %, 79 % and 83 % residual activity under room temperature and vigorous shaking conditions. On the other hand, foam-PDA- and free-OPH showed low stability with residual activities of 62 % and 60 %, respectively. From the comparison of the conversion of immobilized enzymes at the different number of carriers (1, 3, 5) within 12 h catalytic reaction in 20 mL of the reaction solution (Figure 12). It was concluded that the amount of biotransformation of immobilized enzymes is directly proportional to the number of carriers.

Recently, a partially purified OPH was immobilized onto trityl agarose through physical absorption, which was hydrolyzed organophosphate pesticides. However, the major limitation of this immobilized OPH system involved the unavoidable use of the organic solution to improve the solubility of pesticides, resulting in desorption of OPH activity from bioreactor [36]. To avoid such problems, the OPH was immobilized by covalent connection onto four polymer nanofibers grafted to Ni-foam providing a practical method for the organophosphate pesticides to be detoxified. This solid support material was physically stable in a wide variety of environmental conditions and the stability of the immobilized OPH provides the potential for multiple hydrolysis capabilities of organophosphate pesticides.

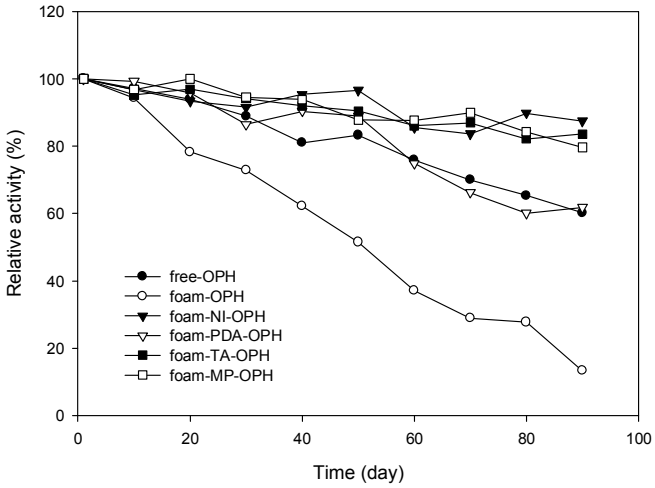

Figure 11. Long-term operational stabilities of free and immobilized OPH at room temperature (25℃).

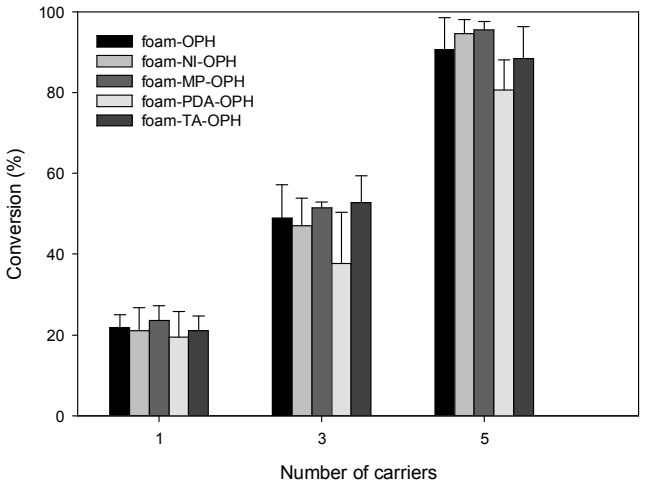

Figure 12. Effect of immobilized OPH carriers on bioconversion.

B. Immobilization of LDC onto various polymer nanofibers for enzyme stabilization

1. Introduction

Polyamide nylon being lighter, softer and more elastic than other fibers, is widely used in the clothing and industrial applications. Many methods have been developed to synthesize the polyamide nylon from fossil fuels. However, the problem associated with such methods is the lack of product's ability to decompose naturally, which causes serious environmental problems. Cadaverine (1, 5-diaminopentane) is a monomer of nylon that can be produced through the decarboxylation reaction of lysine. Cadaverine has been used in the production of polyamide nylon such as PA5, 4, PA5, 6, and PA5, 10, which are bio-based alternatives to conventional petroleum-based polyamines [38-41]. The conversion of lysine to cadaverine is made by LDC under the condition of PLP as a cofactor (Figure 13) [42, 43]. Enzyme immobilization increases biocatalyst stability and reduces the cost of enzymes. As successful cadaverine biosynthesis system has been established, development of reusable and stable enzyme system for repetitive reactions would facilitate economically feasible cadaverine production [39].

Previously, different research groups developed free cells (or whole cells) to immobilize [44]. However, the process has disadvantages such as poor reusability and weak thermal stability. Thus, this study was intended to immobilization of LDC onto foam-PANI, foam-PAMP, foam-PDA and foam-TA for the conversion of lysine to cadaverine. And we analyzed the capacity of four immobilized LDCs to catalyze the conversion of lysine to cadaverine.

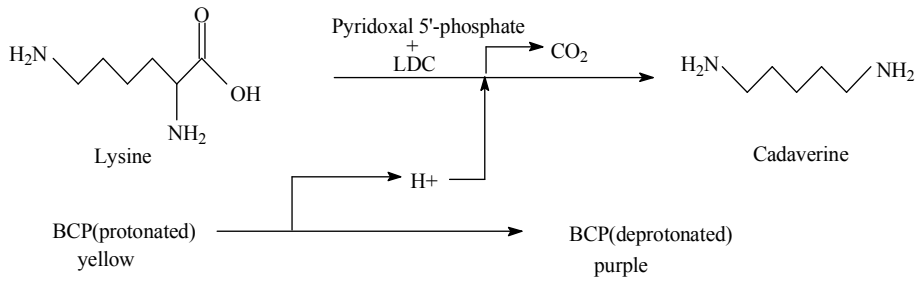

Figure 13. Biotransformation of L-lysine to cadaverine using PLP and LDC.

2. Materials

Anti-foam, PLP, bromocresol purple (BCP), L-lysine, GA, tris (hydroxymethyl) aminomethane were purchased from Sigma-Aldrich. K_2HPO_4, HCl, glucose and glycerol were obtained from Duksan. Yeast extract, KH_2PO_4, and $MgSO_4$ were purchased from Fisher Scientific. NH_4SO_4, NaCl, tryptone, agar were supplied by Becton Dickinson.

Instruments such as sonic dismemberator (Fisher 100 model), fermenter (Biotron Co. Korea), incubator (HANBAEK ST CO. Korea), small high speed refrigerated centrifuge (Hanil, Korea), autoclave (HANBAEK ST CO. Korea), micro themomixer (FINPCR, Korea), deep freezer (DF8517, Il-Shin Bio Co.) were used.

3. Strain and storage

The strain was a recombinant *Pseudomonas aeruginosa* (KCTC 22063) producing LDC. Cells were grown at 37 , 200 rpm for 15 h. 50 % glycerol was added at a ratio of 1:1 (v/v) and mixed completely. Stored in a deep freezer at -70 for further use.

4. Medium composition

The LB medium for activation consisted of tryptone, NaCl, and yeast extract. The fermentation medium was composed of yeast extract, glucose, $(NH_4)_2SO_4$, NaCl, KH_2PO_4, K_2HPO_4, and trace elements $MgSO_4 \cdot 7H_2O$ (Table 2).

Table 2. Media composition for *Pseudomonas aeruginosa* culture for the production of LDC

Component	Concentration	Medium type
Tryptone	1 g/L	LB medium
NaCl	1 g/L	
Yeast extract	0.5 g/L	
Glucose	20 g/L	Fermentation medium
$(NH_4)_2SO_4$	2 g/L	
KH_2PO_4	1 g/L	
K_2HPO_4	1 g/L	
$MgSO_4 \cdot 7H_2O$	2.054 g/L	
NaCl	1 g/L	

5. Production of LDC

a. Culture conditions

A fresh colony from the overnight LB agar plate was inoculated on the LB medium and the cells were grown overnight in a shake flask (37℃, at 200 rpm). The seed culture (100 mL) was inoculated into a 2 L fermenter, and cultured at 37℃, 200 rpm for 15 h.

b. Enzyme activity assays of LDC

(1). Preparation of cell extracts

The cells were harvested by centrifugation (3,000×*g*, 4℃, and 15 min) and concentrated 50 times with 20 mM sodium phosphate buffer (pH 6.0). Cell extracts were prepared by thirty 2 s sonication of washed cell suspensions (2 mL of 20 mM sodium phosphate buffer, pH 6.0) with cooling intervals of 3 s. Cell debris was removed by centrifugation.

(2). Analytical methods

The activities of the free and immobilized LDCs were determined at 42℃ using L-lysine as the substrate, BCP as a color developer and PLP as a coenzyme. The reaction mixture contained 20 mM sodium phosphate buffer (pH 6.0), 1 mM L-lysine, 1 mM PLP, and 70 μM BCP. After adding the free or immobilized LDC, the absorbance was detected at 595 nm with a spectrophotometer.

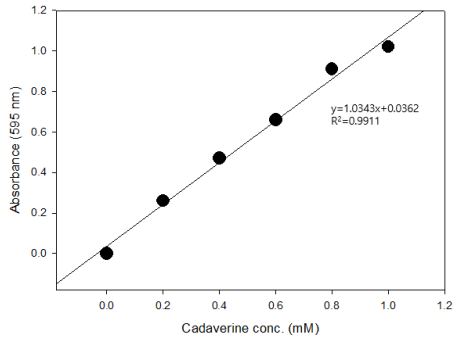

(a)

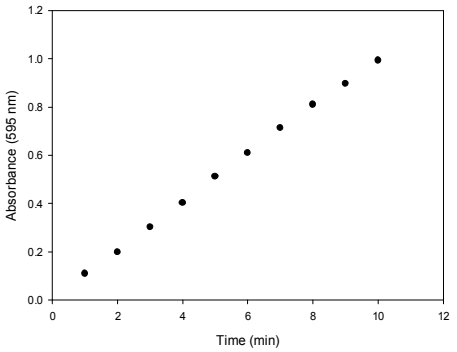

(b)

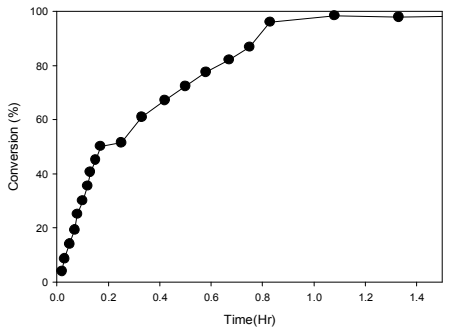

(c)

Figure 14. (a) Standard curve for the determination of cadaverine concentration; (b) activity assay for free LDC; (c) bioconversion with free LDC.

6. LDC immobilization

1 carrier Ni-foam and 1ml crude enzyme solution were mixed with 35 % (w/v) of ammonium sulfate in 1 mL of 20 mM phosphate buffer (pH 6.0) and stirred gently for 30 min at room temperature. Then 2 mL of GA (1 %) as a crosslinker was added and the mixture was agitated for 17 h at 4℃, which can be enough to establish a crosslink between the enzymes. The supernatant was taken to calculate the protein concentrations, measured by the Bradford method, with the enzyme solutions before and after the GA treatment. Subsequently, 1.5 mL of 100 mM tris-HCl (pH 7.9) was added for tris-capping and shaken for 30 min to remove the remaining GA. The immobilized LDC was washed more than 10 times with a 20 mM phosphate buffer (pH 6.0) to remove the free LDCs.

7. Results and discussion

The free and immobilized LDCs relative activities were determined at room temperature under vigorous stirring conditions (Figure 15). The LDC immobilized onto foam-PANI, foam-PAMP, foam-PDA and foam-TA showed only a 0 ~ 6 % decrease in the activity after 3 months of vigorous shaking conditions at room temperature. On the other hand, free-LDC showed low stability with residual activities of 36 %. From the comparison of the conversion of immobilized enzymes at the different number of carriers (1, 3, 5) within 25 h catalytic reaction in 50 mL of the reaction solution (Figure 16), it can be concluded that the amount of biotransformation of immobilized enzymes is directly proportional to the number of carriers.

Immobilized LDC has some advantages over free LDC, such as multiple operations without the free LDC carried away from the downstream process and easier separation from reaction mediums. Alginate was the most widely used polymer for immobilization of the LDC because of its thermostability. Researchers have developed alginate being bivalent ions (Ca^{2+} and Ba^{2+}) immobilization method to immobilize LDC cells [38]. However, Ca-alginate beads were dissolved at high lysine concentration and not stable under different conditions, which might be the sensitivity of the Ca-alginate beads to high diamine concentration. In this work, we used the solid support materials which were physically stable on a wide variety of environmental conditions. Our strategy has many advantages such as reusability, which can be reused many times and result in higher total cadaverine production. Our developed bioprocess is expected to be helpful in developing industrial processes.

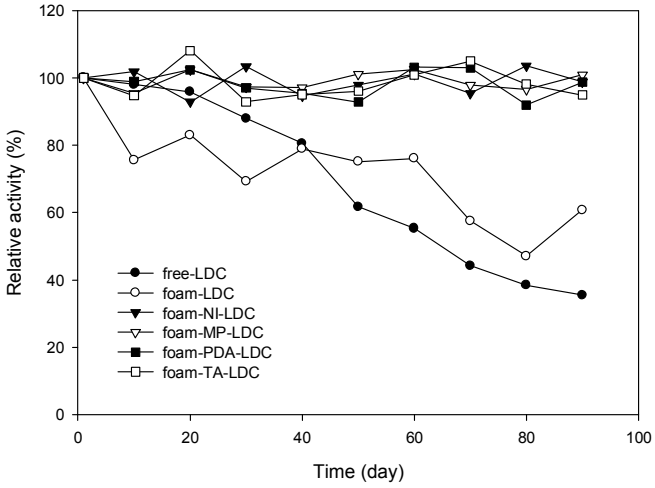

Figure 15. Long-term operational stabilities of free and immobilized LDCs at 42℃.

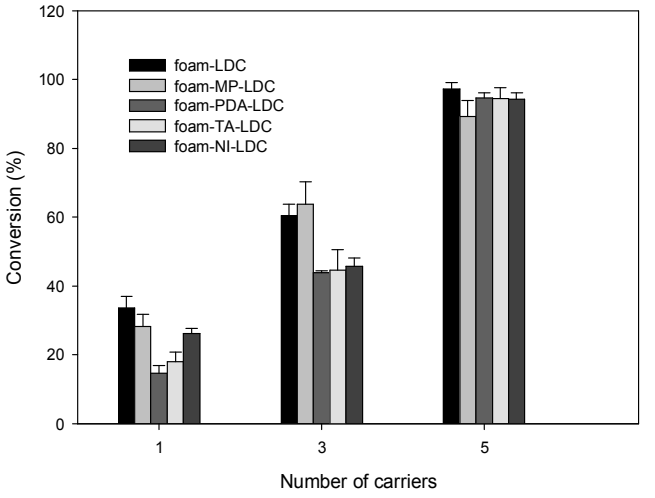

Figure 16. Effect of immobilized LDC carriers on biotransformation.

C. Immobilization of GAD onto various polymer nanofibers for enzyme stabilization

1. Introduction

GAD catalyzes the conversion of glutamic acid to GABA by consuming one proton and using PLP as a cofactor (Figure 17) [45]. GABA is a non-proteinaceous amino acid and is widely used in the chemical industry where it can be employed as a precursor for biodegradable polymers as an intermediate to pyrrolidone to synthesize polymer nylon 4. It has also been used in the pharmaceutical and food industry, where it serves as an inhibitor of neurotransmission with diuretic and hypotensive effects [46]. Because of these beneficial functions, there have been many attempts to synthesize GABA using biological (microbial fermentation) or chemical methods for their deployment in pharmaceutical, foods, and other related industries [47].

GAD is the key enzyme that catalyzes the GABA production [47] and immobilized GAD may be additionally employed to recycle GAD for easy downstream processing and cost efficiency [46]. Up till now, although some immobilization methods, such as using the cellulose binding domain [45], bacterial cellulose membrane [48] and porous silica beads [49] were attempted, few economical, and the capacity was limited. Therefore, in this work, we analyzed the capacity of four immobilized GADs to catalyze the conversion of glutamic acid to GABA.

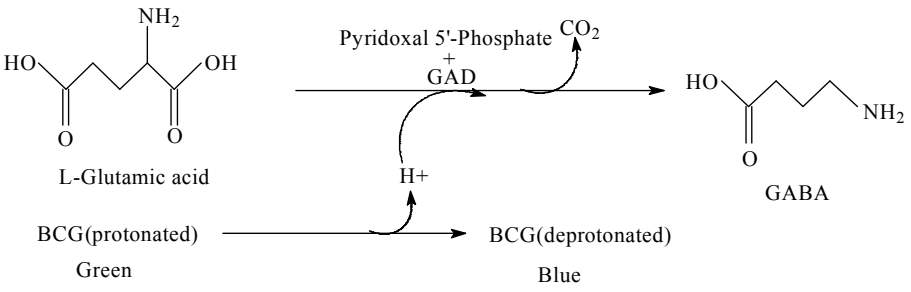

Figure 17. Biotransformation of L-glutamic acid to GABA using GAD.

2. Materials

Yeast extract, KH_2PO_4, H_2SO_4, $MgSO_4$, $CaCl_2$, $CoCl_2$, $FeSO_4$, $Na_2HPO_4 \cdot 7H_2O$ were obtained from Fisher Scientific. Anti-foam, PLP, bromocresol green (BCG), GA, tris (hydroxymethyl) aminomethane were purchased from Sigma-Aldrich. NH_4Cl, NaCl, MSG, tryptone, glucose, agar, IPTG, glycerol were supplied by Baker.

Instruments such as sonic dismemberator (Fisher 100 model), fermenter (Biotron Co. Korea), and incubator (HANBAEK ST CO. Korea), small high speed refrigerated centrifuge (Hanil, Korea), autoclave (HANBAEK ST CO. Korea), deep freezer (DF8517, Il-Shin Bio Co.) were used.

3. Strain and Storage

The strain was a recombinant *Escherichia coli* producing GAD purchased from Kwangwoom University. Cells were grown at 37 , 200 rpm until the OD_{600} reached 0.6 ~ 0.8. 50 % glycerol was added at a ratio of 1:1 (v/v) and mixed completely. Store in a deep freezer at -70 for further use.

4. Medium composition

The LB medium for activation consisted of tryptone, NaCl, and yeast extract. The fermentation medium was composed of yeast extract, glucose, MSG, NH_4Cl, NaCl, KH_2PO_4, Na_2HPO_4, and trace elements $CaCl_2$, $CoCl_2$, $MgSO_4$ (Table 3).

Table 3. Media composition for recombinant *Escherichia coli* culture for the production of GAD

Component	Concentration	Medium type
Tryptone	1 g/L	LB medium
NaCl	1 g/L	
Yeast extract	0.5 g/L	
Glucose	40 g/L	Fermentation medium
KH_2PO_4	3 g/L	
NaCl	0.5 g/L	
NH_4Cl	1 g/L	
Na_2HPO_4	6.78 g/L	
Yeast Extract	2 g/L	
$MgSO_4$	1 mM/L	
$CaCl_2$	0.5 mM/L	
$CoCl_2$	0.5 mM/L	
MSG	20 g/L	

5. Production of GAD

a. Culture conditions

A fresh colony from the overnight LB agar plate was inoculated on the LB medium and the cells were grown overnight in a shake flask (37℃, at 200 rpm). The seed culture(100 mL) was inoculated into a 2 L fermenter and cultured at 37℃, 200 rpm until the OD_{600} reached 5 (Exponential growth period). For induction, IPTG (24 mg/mL) was added and the culture was shaken for further 16 h at 16℃， 200 rpm.

b. Enzyme activity assays of GAD

(1). Preparation of cell extracts

The cells were harvested by centrifugation (3,000×*g*, 4℃, and 15 min) and concentrated 100 times with 0.5 M sodium acetate buffer (pH 5.0). Cell extracts were prepared by thirty 2 s sonication of washed cell suspensions (2 mL of 0.5 M sodium acetate buffer, pH 5.0) with cooling intervals of 3 s. Cell debris was removed by centrifugation.

(2). Analytical methods

The activities of the free and immobilized GADs were determined at 37℃ using 1 mM MSG as the substrate, BCG as a color developer and PLP as a coenzyme. The reaction mixture contained 0.5 M sodium acetate buffer (pH 5.0), 1 mM MSG, 0.5 mM PLP, and 70 μM BCG. After adding the free or immobilized GAD, the absorbance was detected at 620 nm with a spectrophotometer.

(3). GABA derivatization and HPLC-UV analytical method

Sample treatment: 200 μL of GABA containing microbial transformation solution was taken in a 1.5 mL centrifuge tube, and then 800 μL of 10 % trichloroacetic acid solution was added. The solution was allowed to react in a 40℃ water bath for 2 h, and then centrifuged for 10 min at 1000 rpm, and the supernatant was diluted in various concentrations for standby.

Derivative method: samples (0.5 mL) or GABA standard solution (40 μL) was mixed with 0.9

mL of $NaHCO_3$ solution (1 mL with pH 9.5) and 1mL of the freshly prepared 1-fluoro-2, 4-dinitrobenzen (DNFB) (4 mmol/L in acetone). The mixture was heated at 55℃ for 1 h to derivatize GABA. Afterwards, the reaction was terminated by cooling the mixture. The final samples were filtered through a 0.22 μm nylon filter before HPLC analysis.

HPLC system coupled with a Luna C18 column (250× 4.6 mm, 5 μm, phenomenex, USA) was used to analyse the GABA content in the GAD catalytic reaction with an injection volume of 10 μL. The mobile phase consisted of (A) methanol and (B) tetrahydrofuran-methanol-0.05 mol/L sodium acetate (5:75:20, v/v/v). The gradient programme was as follows: 0 ~ 8 min, 30% A isocratic; 8 ~ 20 min, 30% A to 60% A; 20 ~ 25 min, 60% A to 100% A; 25 ~ 30 min, 100% A isocratic; 30 ~ 35 min, 100% A to 30% A; and 35 ~ 40 min, 30% A isocratic. The wavelength was 254 nm, and the flow rate was 1.0 mL/min [50].

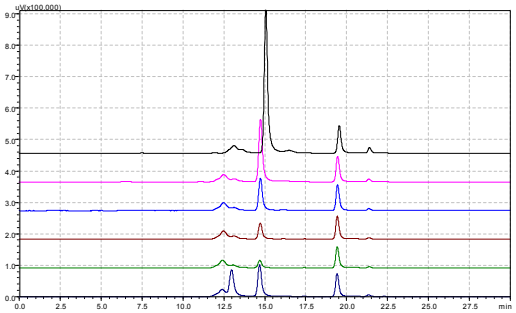

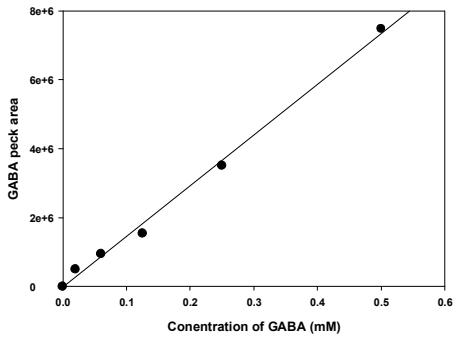

(a)

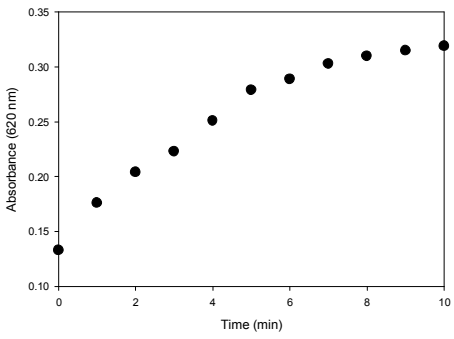

(b)

Figure 18. (a) Standard curve for the determination of GABA; (b) activity assay for free GAD.

6. GAD immobilization

1 carrier Ni-foam and 1mL crude enzyme solution were mixed with 35 % (w/v) of ammonium sulfate in 1 mL of a 0.5 M sodium acetate (pH 5.0) and stirred gently for 30 min at room temperature. Then 2 mL of a glutaraldehyde solution (1 %) as a crosslinker was added. The mixture was agitated for 17 h at 4℃, which can be enough to establish a crosslink between the enzymes. The supernatant was taken to calculate the protein concentrations, measured by the Bradford method, with the enzyme solutions before and after the glutaraldehyde treatment. Subsequently, 1.5 mL of 100 mM tris-HCl (pH 7.9) was added for tris-capping and shaken for 30 min to remove the remaining GA. The immobilized GAD was washed more than 10 times with a 0.5 M sodium acetate (pH 5.0) to remove the free GADs.

7. Results and discussion

The free and immobilized GADs relative activities were determined at room temperature under vigorous stirring conditions (Figure 19). The GAD immobilized onto foam-PANI, foam-PAMP and foam-TA showed above 89 %, 88 % and 81 % residual activity under vigorous shaking conditions room temperature. On the other hand, foam-PDA-GAD and free-GAD showed low stability with residual activities of 42 % and 19 %, respectively. From the comparison of the conversion of immobilized enzymes at the different number of carriers (1, 3, 6) within 8 h catalytic reaction in 20 mL of the reaction solution (Figure 20), it can be concluded that the amount of biotransformation of immobilized enzymes is directly proportional to the number of carriers.

In this work, the free GAD was unstable under experimental conditions. The stability result of the immobilized GAD provides a simple and low-cost method for the large scale production of GABA. Moreover, compared with fixing GAD to cellulose binding domain (CBD) [46], one-step immobilization without GAD purification step might be useful for industrial applications. Reusing of GAD and reversible immobilization might be potentially applicable to large-scale production of GABA.

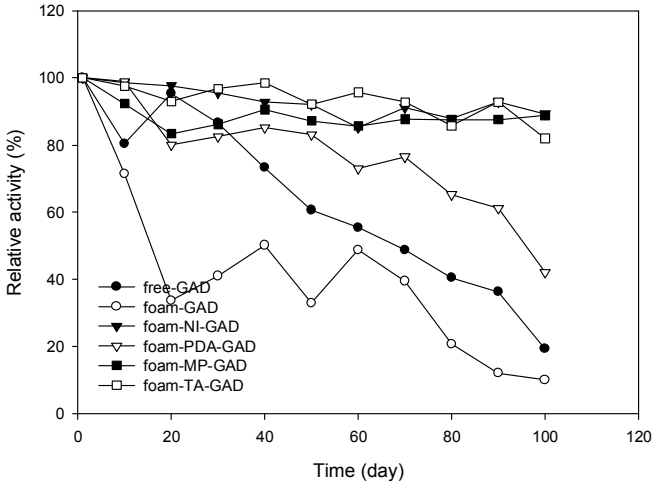

Figure 19. Long-term operational stabilities of free and immobilized GADs at room temperature (25℃).

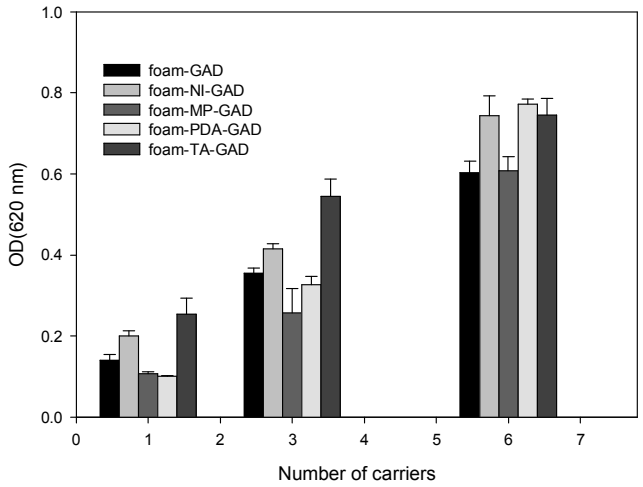

Figure 20. Effect of immobilized GAD carriers on biotransformation.

D. Immobilization of ω-transaminase onto various polymer nanofibers for enzyme stabilization

1. Introduction

Enantiopure amines are essential chiral building blocks for the synthesis of a wide variety of active pharmaceutical ingredients. Chemical synthesis of these compounds usually employs transition metal catalysts of relatively high toxicity and may require harsh reaction conditions. In recent years, there has been a growing interest in ω-transaminases (ω-TA) which is a PLP dependent enzyme. ω-TA plays a very important role in the synthesis of non-natural amino acids and chiral amines [51-56]. ω-TA have been used in the preparation of several pharmaceutically relevant compounds, like 3-aryl-γ-aminobutyric acid derivatives, sitagliptin and valinol [57].

However, ω-TA is mostly restricted by its low stability, high production cost and complicated recyclability [58]. In order to overcome these problems, some efforts have been made for the immobilization of ω-TA. These efforts include entrapping ω-TA into calcium alginate [59], binding with chitosan covalently [60], and immobilization of ω-TA onto Sol-gel/Celite 545 [61], SEPABEADS EXE 120 [62] demonstrated its good capability and recyclability.

In this study, four polymer nanofibers were prepared and applied for the immobilization of ω-TA. The immobilized ω-TA was characterized by enzymatic stability and recyclability, in order to provide more possibilities for the immobilization of ω-TA. Here, acetophenone was used as the amine acceptor, and L-alanine was used as the amine donor for the transamination reaction (Figure 21).

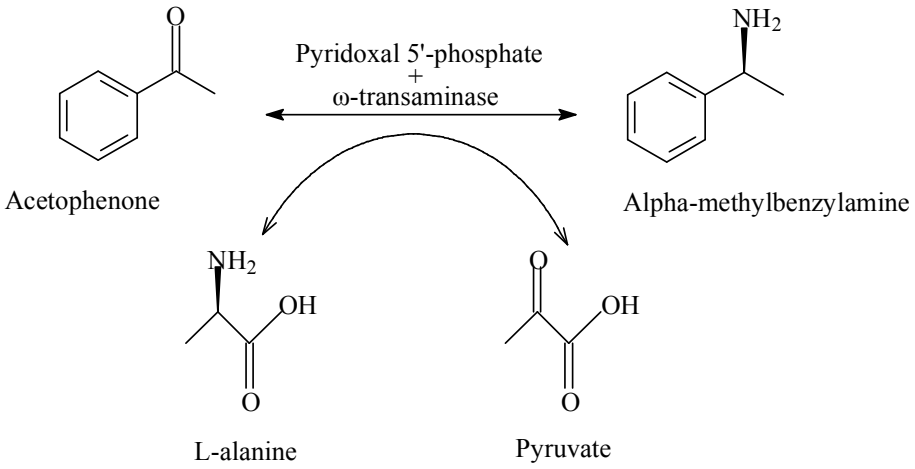

Figure 21. Reaction mechnism of chiral amines using ω-transaminase.

2. Materials

Yeast extract, KH_2PO_4, K_2HPO_4, NH_4SO_4, HCl, $MgSO_4$, $Na_2HPO_4 \cdot 7H_2O$ were obtained from Fisher Scientific. Acetophenone, L-alanine, sodium pyruvate, anti-foam, PLP, GA, tris (hydroxymethyl) aminomethane were purchased from Sigma-Aldrich. NH_4Cl, NaCl, tryptone, glucose, agar, IPTG, glycerol were supplied by Baker.

Instruments such as sonic dismemberator (Fisher 100 model), fermenter (Biotron Co. Korea), and incubator (HANBAEK ST CO. Korea), small high speed refrigerated centrifuge (Hanil, Korea), autoclave (HANBAEK ST CO. Korea), deep freezer (DF8517, Il-Shin Bio Co.) were used.

3. Strain and Storage

The strain was a wild-type *Chromobacterium violaceum* DSM30191 producing ω-TA purchased from the Korean Collection for Type Cultures. Cells were grown at 26 , 200 rpm for 1 ~ 2 day. 50 % glycerol was added at a ratio of 1:1 (v/v) and mixed completely. Store in a deep freezer at -70 for further use.

4. Medium composition

The nutrient agar medium for activation consisted of beef extract and peptone. The fermentation medium was composed of yeast extract, glucose, $(NH_4)_2SO_4$, NaCl, KH_2PO_4, K_2HPO_4, acetophenone and trace elements $MgSO_4 \cdot 7H_2O$ (Table 4).

Table 4. Media composition for *Chromobacterium violaceum* culture for the production of ω-TA

Component	Concentration	Medium type
Beef extract	3 g/L	Primary seed culture medium (Nutrient Agar)
Peptone	5 g/L	
Glucose	20 g/L	Fermentation medium
$(NH_4)_2SO_4$	2 g/L	
KH_2PO_4	1 g/L	
K_2HPO_4	1 g/L	
$MgSO_4 \cdot 7H_2O$	2.054 g/L	
NaCl	1 g/L	
Acetophenone	0.17 M	

5. Production of ω-TA

a. Culture conditions

A fresh colony from the overnight LB agar plate was inoculated on the LB medium and the cells were grown overnight in a shake flask (26℃, at 200 rpm). The seed culture (100 mL) was inoculated into a 2 L fermenter, and cultured at 26℃, 200 rpm for 15 h.

b. Enzyme activity assays of ω-TA

(1). Preparation of cell extracts

The cells were harvested by centrifugation (3,000×*g*, 4℃, and 15 min) and concentrated 100 times with 50 mM phosphate buffer (pH 7.5). Cell extracts were prepared by twenty 2 s sonication of washed cell suspensions (2 mL of 50 mM phosphate buffer, pH 7.5) with cooling intervals of 3 s. Cell debris was removed by centrifugation.

(2). Analytical methods

The activities of the free and immobilized ω-TAs were determined at 30℃ using 1 mM acetophenone and 10 mM L-alanine as the substrate, PLP as a coenzyme. The reaction mixture contained 50 mM phosphate buffer (pH 7.5), 1 mM acetophenone and 10 mM L-alanine, and 0.5 mM PLP. After adding the free or immobilized ω-TA, the reduction of acetophenone was analyzed by GC. The analysis was performed on Shimadzu-10A with FID detector and DB-5ms column (60 m×0.25 mm×0.25 um) using N_2 carrier gas (injector: 250℃, detector: 250℃, head pressure: 12 psi, split ratio: 30:1).

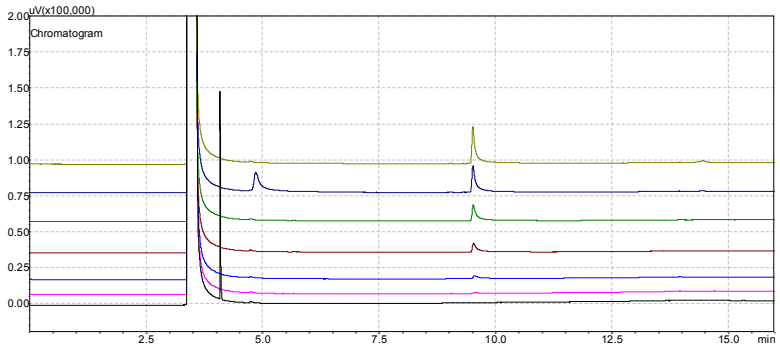

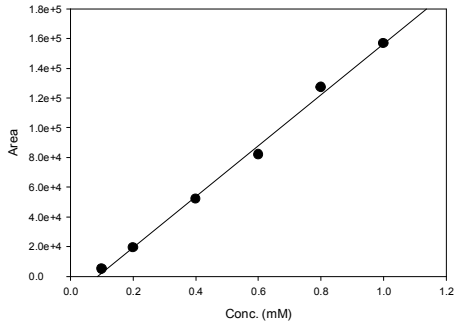

(a)

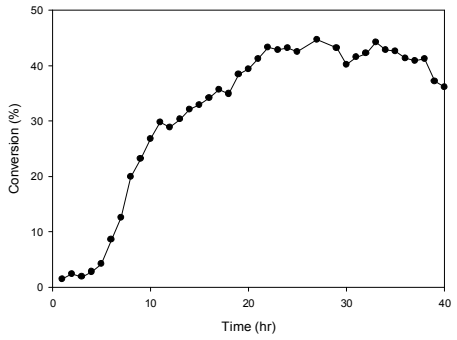

(b)

Figure 22. (a) GC standard curve; (b) bioconversion with free ω-TA.

6. ω-TA immobilization

1 carrier Ni-foam and 1 mL crude enzyme solution were mixed with 35 % (w/v) of ammonium sulfate in 1 mL of a 50 mM phosphate buffer (pH 7.5) and stirred gently for 30 min at room temperature. Then 1 mL of a GA (1 %) as a crosslinker was added. The mixture was agitated for 17 h at 4℃, which can be enough to establish a crosslink between the enzymes. The supernatant was taken to calculate the protein concentrations, measured by the Bradford method, with the enzyme solutions before and after the GA treatment. Subsequently, 1.5 mL of 100 mM tris-HCl (pH 7.9) was added for tris-capping and shaken for 30 min to remove the remaining GA. The immobilized ω-TA was washed more than 10 times with 50 mM phosphate buffer (pH 7.5) to remove the free ω-TAs.

7. Results and discussion

The free and immobilized ω-TAs relative activities were determined at room temperature under vigorous stirring conditions (Figure 23). The ω-TA immobilized onto foam-PANI and foam-TA showed above 97 %, and 88 % residual activity under room temperature and vigorous shaking conditions. On the other hand, foam-PAMP-, foam-PDA- and free-(ω-TA) showed low stability with residual activities of 35 %, 16 % and 39 %, respectively. From the comparison of the conversion of immobilized enzymes at the different number of carriers (1, 3, 6) within 48 h catalytic reaction in 30 mL of the reaction solution (Figure 24), it can be concluded that the amount of biotransformation of immobilized enzymes is directly proportional to the number of carriers.

Activity loss of □-TA upon immobilization might be due to the combination of various factors. Prior research on immobilized enzymes has indicated that properties of immobilization surface play a very important role in the enzyme activity [63]. The immobilized □-TA on foam-PANI and foam-TA were successfully used for the repetitive reaction and showed good stability. It is necessary to improve the stability of the immobilized □-TA first by increasing the activity of the enzyme in further research.

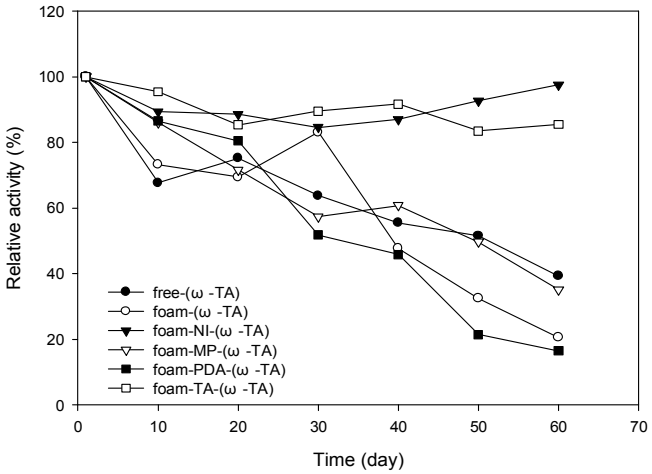

Figure 23. Long-term operational stabilities of free and immobilized ω-TAs at room temperature (25℃).

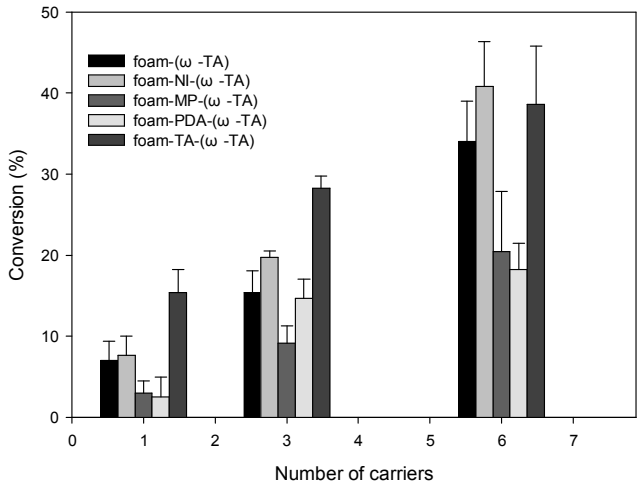

Figure 24. Effect of immobilized ω-TA carriers on biotransformation.

Ⅲ. Application of foam-PANI-, foam-PAMP-, foam-PDA- and foam-TA- enzymes for biotransformation using CSTR

1. Introduction

Figure 25. Displays the schematic diagram of the enzyme catalytic reaction system for performance analysis of immobilized OPH, LDC, GAD and ω-TA in continuous stirred tank reactor (CSTR). The system consists of three sections: feed system, enzyme reactor and sample collection system. The feed system includes a pump and the flow meters, which can adjust and control the inlet concentration. The enzyme reactor was made of reaction vial (15 mm inside diameter and 50 mm in length) with precise temperature control. The porous nickel sheet (4 cm^2) that was coated with polymer nanofibers (PANI, PAMP, PDA and TA) was installed inside the reaction vial. The collection system consists of an automatic collector and pump, which can analyze the content of the product.

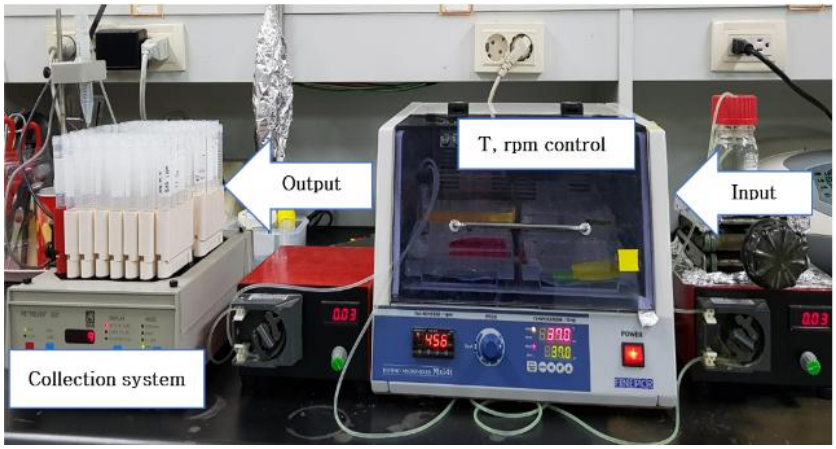

Figure 25. Continuous stirred tank reactor (CSTR).

2. Biotransformations with the immobilized enzymes using CSTR

a. Degradation of paraxon with immobilized OPH in CSTR

The paraxon was dissolved in a buffer solution of CHES (125 mM, pH 9.0). The 2 biocatalyst-filled nickel sheets where pre-washed by CHES buffer (0.03 mL/min for 60 min) followed by pumping the substrate solution through the reaction vial (2 mL) at a flow rate (0.03 mL/min) at 25℃. The reaction liquid collected every hour was measured by spectrophotometer as described earlier.

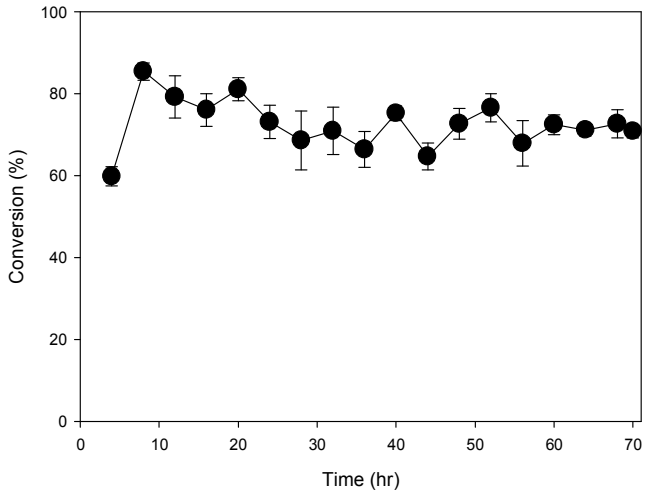

Figure 26. Continuous paraxon hydrolysis using foam-PANI-OPH at 25 .

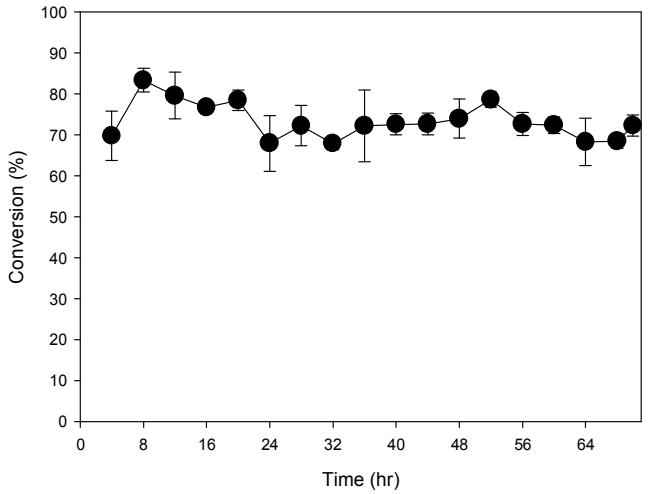

Figure 27. Continuous paraxon hydrolysis using foam-PAMP-OPH at 25 .

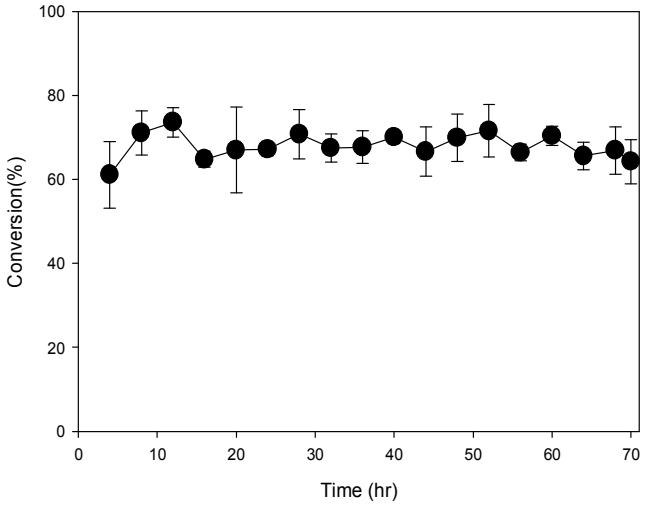

Figure 28. Continuous paraxon hydrolysis using foam-PDA-OPH at 25 .

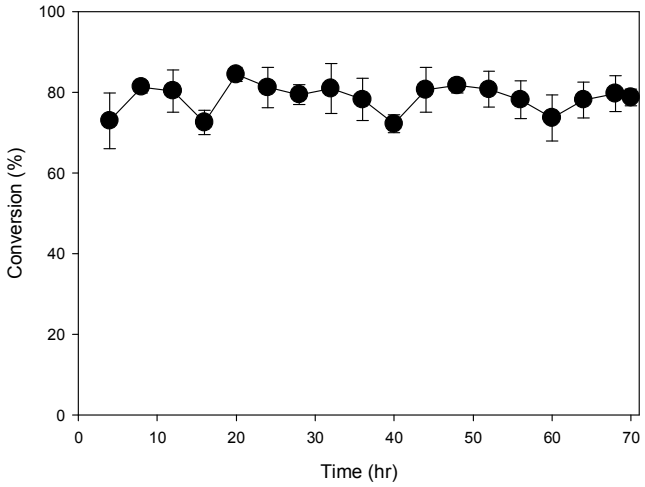

Figure 29. Continuous paraxon hydrolysis using foam-TA-OPH at 25 .

b. Lysine decarboxylation with immobilized LDC in CSTR

The lysine was dissolved in sodium phosphate buffer (20 mM, pH 6.0) containing PLP (1 mM) and BCP (70 μM). The 2 biocatalyst-filled nickel sheets were pre-washed by sodium phosphate buffer (0.03 mL/min for 60 min) followed by pumping the substrate solution through the reaction vial (2 mL) at a flow rate (0.03 mL/min) at 42℃. The reaction liquid collected every hour was measured by spectrophotometer as described earlier.

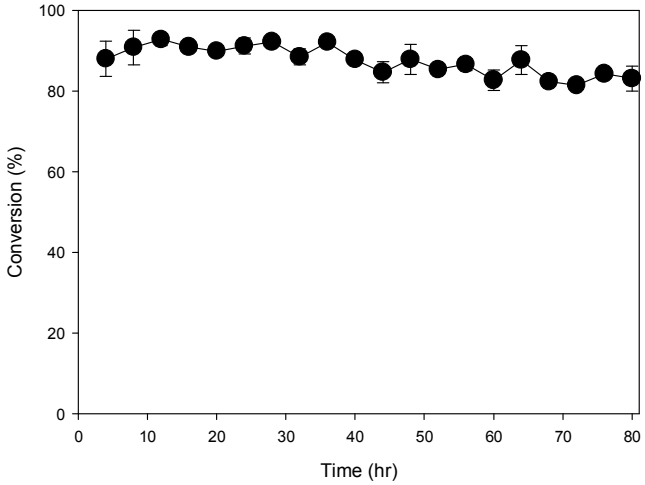

Figure 30. Continuous lysine decarboxylation using foam-PANI-LDC at 42 .

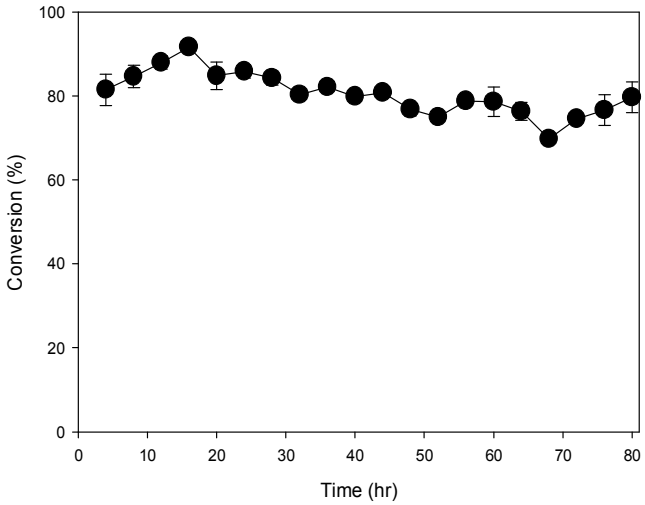

Figure 31. Continuous lysine decarboxylation using foam-PAMP-LDC at 42 .

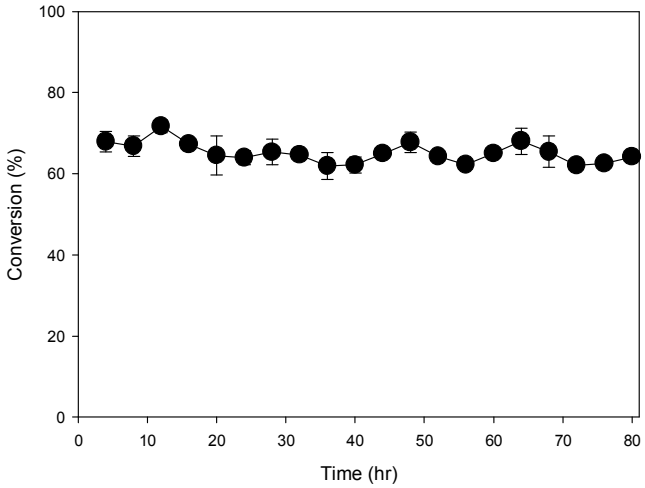

Figure 32. Continuous lysine decarboxylation using foam-PDA-LDC at 42 .

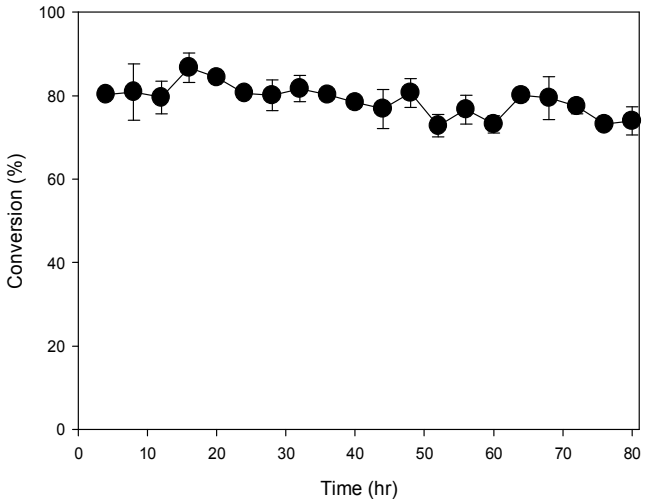

Figure 33. Continuous lysine decarboxylation using foam-TA-LDC at 42 .

c. Synthesis of GABA with immobilized GAD in CSTR

The MSG was dissolved in sodium acetate buffer (0.5 M, pH 5.0) containing PLP (0.5 mM). The 4 biocatalyst-filled nickel sheets were pre-washed by sodium acetate buffer (0.03 mL/min for 60 min) followed by pumping the substrate solution through the reaction vial (2 mL) at a flow rate (0.03 mL/min) at 37℃. The reaction liquid collected every hour was measured by HPLC as described earlier.

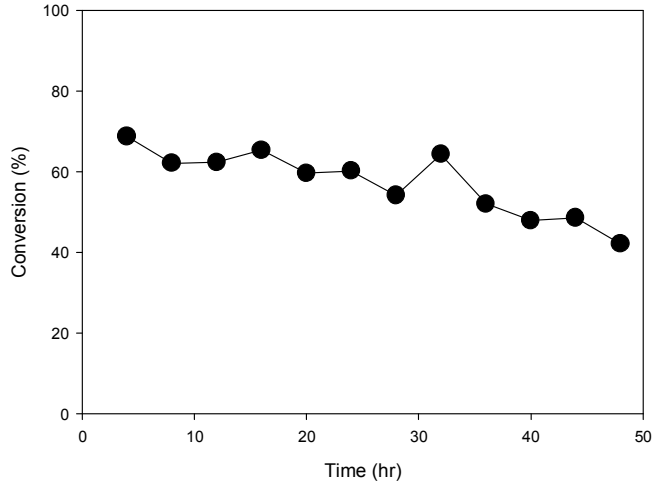

Figure 34. Synthesis of GABA using foam-PANI-GAD at 37 .

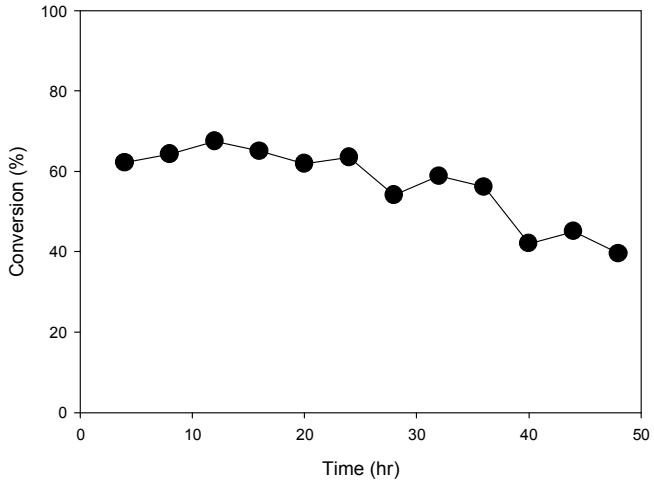

Figure 35. Synthesis of GABA using foam-PAMP-GAD at 37 .

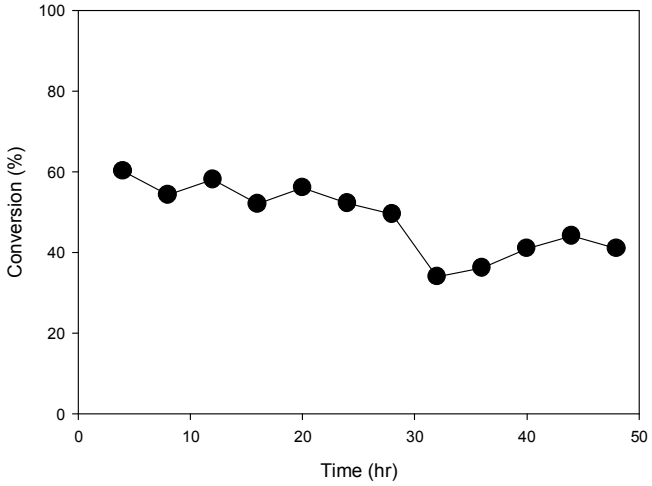

Figure 36. Synthesis of GABA using foam-PDA-GAD at 37 .

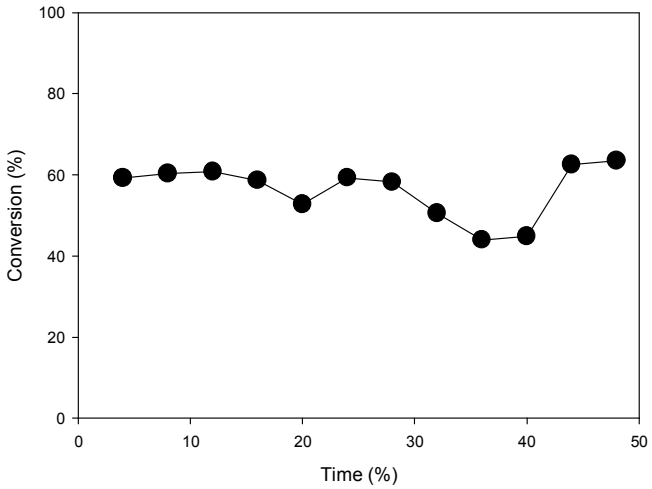

Figure 37. Synthesis of GABA using foam-TA-GAD at 37 .

d. Batch synthesis of chiral amines using recycled immobilized ω-TA

The acetophenone (1 mM) was dissolved in phosphate buffer (50 mM, pH 7.5) containing PLP (0.5 mM) and L-alanine (10 mM). The immobilized ω-TA was recycled 10 times after transamination reaction in reaction vial (2 mL) at 30℃. The reaction liquid collected every 24 hours was measured by GC as described earlier.

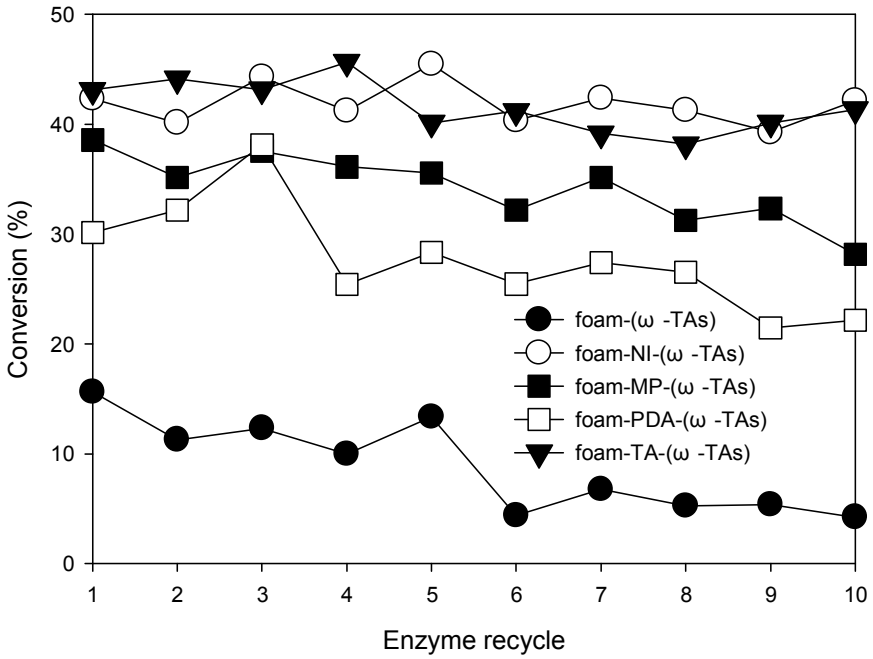

Figure 38. Synthesis of chiral amines using recycled immobilized ω-TA.

3. Results and discussion

Immobilization of enzymes onto foam-PANI, foam-PAMP, foam-PDA, and foam-TA creates promising biocatalysts for biotransformation in continuous-flow and batch mode reactions. Compared to the immobilized OPH [33, 34], LDC [38, 49], GAD [45-47], and □-TA [57, 58, 64] reported in previous publications, the easy-to-use immobilized enzymes biocatalysts showed the enhance stability and proved to be stable even in the long-term continuous processes. In future, the further investigation would be required to achieve more economical and more active process by incorporation of inexpensive stability-enhancing immobilization carriers.

Ⅳ. Conclusion

The immobilization of the OPH, LDC, GAD and ω-TA onto four polymer nanofibers provides effective methods for enzyme stabilization and recycle. It is the first report on the immobilization of OPH, LDC, GAD and ω-TA using four polymer nanofibers, namely, foam-PANI, foam-PAMP, foam-PDA, and foam-TA.

Enzymes immobilized on foam-PANI, foam-PAMP, and foam-TA showed higher activity and stability. As shown in Figure 39, foam-PANI, foam-PAMP, and foam-TA have a large surface area and they can be easily coated with enzymes. The immobilization yield (IY, %) (Table 5) of the foam-PDA is also relatively low. The PDA grafted Ni-foam does not have enough space for enzyme immobilization. This might prevent the substrate from diffusing freely toward the immobilized enzyme inside the nickel foam, but other supporting materials do not have such a diffusion problem.

In conclusion, the enzymes immobilized on foam-PANI, foam-PAMP, foam-PDA, and foam-TA showed improved stability and recyclability. The immobilized enzymes were easily recovered and recycled after reaction and could be applied for the scale-up production. In the future, further scale-up investigation is required to achieve a more economically feasible process in terms of enhanced stability.

Table 5. Immobilization yield and stabilities of immobilized enzymes on various polymer nanofibers;

Enzyme	Polymer Nanofiber									
	foam		foam-PANI		foam-PAMP		foam-PDA		foam-TA	
	IY (%)	Activity Retention after 90th day (%)	IY (%)	Activity retention after 90th day (%)	IY (%)	Activity retention after 90th day (%)	IY (%)	Activity retention after 90th day (%)	IY (%)	Activity retention after 90th day (%)
OPH	0.64	13.37	0.65	87.49	0.6	79.65	0.58	61.83	0.69	83.57
LDC	0.68	60.8	0.72	98.85	0.66	100.86	0.62	98.76	0.71	94.9
GAD	0.73	10.11	0.67	89.26	0.7	88.75	0.54	42.09	0.74	81.99
ω-TA	0.65	20.5	0.67	97.56	0.64	35.09	0.56	16.47	0.69	85.47

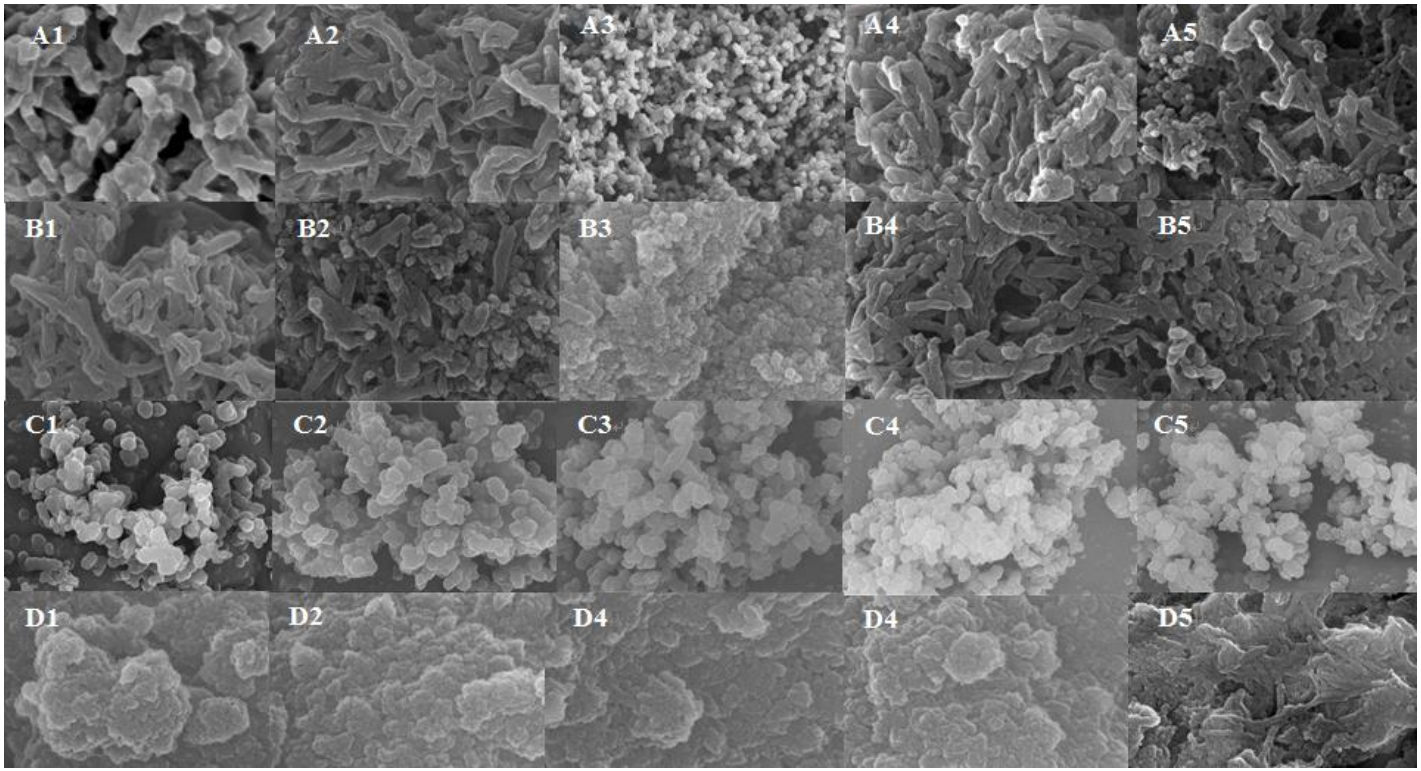

Figure 39. SEM images at 100 nm of (A1-A5) foam-NI, foam-NI-OPH, foam-NI-LDC, foam-NI-GAD, foam-NI-(ω-TA); (B1-B5) foam-MP, foam-MP-OPH, foam-MP-LDC, foam-MP-GAD, foam-MP-(ω-TA); (C1-C5)foam-PDA, foam-PDA-OPH, foam-PDA-LDC, foam-PDA-GAD, foam-PDA-(ω-TA); (D1-D5)foam-TA, foam-TA-OPH, foam-TA-LDC, foam-TA-GAD, foam-TA-(ω-TA).

REFERENCES

1. Homaei, A.A. et al., Enzyme immobilization: an update. Journal of Chemical Biology, 2013. **6**(4): p. 185-205.

2. Cao, L., L. van Langen, and R.A. Sheldon, Immobilised enzymes: carrier-bound or carrier-free? Current Opinion in Biotechnology, 2003. **14**(4): p. 387-394.

3. Jia, H. et al., Immobilization of ω-transaminase by magnetic PVA-Fe_3O_4 nanoparticles. Biotechnology Reports, 2016. **10**: p. 49-55.

4. Bhadra, S. et al., Progress in preparation, processing and applications of polyaniline. Progress in Polymer Science, 2009. **34**(8): p. 783-810.

5. Boeva, Z.A. and V.G. Sergeyev, Polyaniline: synthesis, properties, and application. Polymer Science Series C, 2014. **56**(1): p. 144-153.

6. Ramazan, A. and Waseem S. K., Electrospun nanofibers for nanosensor and biosensor applications. Synthesis and Application of Electrospun Nanofibers, 2019. **9**: p. 175-196.

7. Yusoff, N., Graphene–polymer modified electrochemical sensors, in graphene-based electrochemical sensors for biomolecules. 2019, Elsevier. p. 155-186.

8. Baker, C.O. et al., Polyaniline nanofibers: broadening applications for conducting polymers. Chemical Society Reviews, 2017. **46**(5): p. 1510-1525.

9. Yiu, H.H. and M.A. Keane, Enzyme–magnetic nanoparticle hybrids: new effective catalysts for the production of high value chemicals. Journal of Chemical Technology & Biotechnology, 2012. **87**(5): p. 583-594.

10. Zhang, Z., M. Wan, and Y. Wei, Electromagnetic functionalized polyaniline nanostructures. Nanotechnology, 2005. **16**(12): p. 2827.

11. Lee, G., J. Kim, and J.-H. Lee, Development of magnetically separable polyaniline nanofibers for enzyme immobilization and recovery. Enzyme and Microbial Technology, 2008. **42**(6): p. 466-472.

12. Sozeri, H. et al., Polyaniline (PANI)–Co0. 5Mn0. 5Fe_2O_4 nanocomposite: Synthesis, characterization and magnetic properties evaluation. Ceramics International, 2013. **39**(5): p. 5137-5143.

13. Dai, L.F., The preparation of PPy/PDA nanocomposites material and its interaction with osteoblasts. Scientia Silvae Sinicae, 2016. **41**(6): p. 157-189.

14. Batul, R. et al., Recent progress in the biomedical applications of polydopamine nanostructures. Biomaterials Science, 2017. **5**(7): p. 1204-1229.

15. Seok, S. et al., Dopamine-induced Pt and N-doped carbon@ silica hybrids as high-performance anode catalysts for polymer electrolyte membrane fuel cells. RSC Advances, 2014. **4**(80): p. 42582-42584.

16. Li, D.D. et al., Progress in the application of tannic acid to the functional materials. Applied Surface Science, 2017. **9**: p. 10-20

17. He, Z.E. et al., Application and research progress on polyphenols material. Chemical Society Reviews, 2017. **37**(6): p. 919-924.

18. Ejima, H. et al., One-step assembly of coordination complexes for versatile film and particle engineering. Science, 2013. **341**(6142): p. 154-157.

19. Liping, Z. et al., The present conditions and development trend of plant polyphenols research. Scientia Silvae Sinicae, 2005. **41**(6): p. 157.

20. Jin, L. et al., Immobilization of lactase onto various polymer nanofibers for enzyme stabilization and recycling. J. Microbiol. Biotechnol, 2015. **25**(8): p. 1291-1298.

21. Jiang, X., Y. Wang, and M. Li, Selecting water-alcohol mixed solvent for synthesis of polydopamine nano-spheres using solubility parameter. Scientific Reports, 2014. **4**: p. 6070.

22. Zhang, X. et al., Co-deposition of tannic acid and diethlyenetriamine for surface hydrophilization of hydrophobic polymer membranes. Applied Surface Science, 2016. **360**: p. 291-297.

23. Guan, H. et al., Polyaniline nanofibers obtained by interfacial polymerization for high-rate supercapacitors. Electrochimica Acta, 2010. **56**(2): p. 964-968.

24. Du, Y., K. Cai, and S.Z. Shen, Facile preparation and characterization of graphene nanosheet/polyaniline nanofiber thermoelectric composites. Functional Materials Letters, 2013. **6**(05): p. 1340002.

25. Kumar, A. et al., Synthesis and characterization of hybrid PANI/MWCNT nanocomposites for EMI applications. Polymer Composites, 2018. **39**(11): p. 3858-3868.

26. Rafeeq, S.N. and W.Z. Khalaf, Preparation, characterization and electrical conductivity of doped polyaniline with (HCL and P-TSA). Engineering and Technology Journal, 2015. **33**(7 Part (B) Scientific): p. 1220-1231.

27. Bachhav, S. and D. Patil, Synthesis and characterization of polyaniline-multiwalled carbon nanotube nanocomposites and its electrical percolation behavior. Am J Mater Sci, 2015. **5**(4): p. 90-95.

28. Luo, H. et al., Facile synthesis of novel size-controlled antibacterial hybrid spheres using silver nanoparticles loaded with poly-dopamine spheres. RSC Advances, 2015. **5**(18): p. 13470-13477.

29. Batul, R. et al., Synthesis of polydopamine nanoparticles for drug delivery applications. Microscopy and Microanalysis, 2018. **24**(S1): p. 1758-1759.

30. Çakar, S. and M. Özacar, Fe–tannic acid complex dye as photo sensitizer for different morphological ZnO based DSSCs. Spectrochimica Acta Part A: Molecular and Biomolecular Spectroscopy, 2016. **163**: p. 79-88.

31. Li, Y. et al., Iron-tannic acid nanocomplexes: facile synthesis and application for removal of methylene blue from aqueous solution. Digest Journal of Nanomaterials & Biostructures (DJNB), 2016. **11**(4): p. 197-205.

32. Alonso, P.E.d.G., Alternative synthesis methods of electrically conductive bacterial cellulose-polyaniline composites for potential drug delivery application. Microscopy and Microanalysis, 2017. **24**: p. 758-759.

33. Wang, J., D. Bhattacharyya, and L.G. Bachas, Orientation specific immobilization of organophosphorus hydrolase on magnetic particles through gene fusion. Biomacromolecules, 2001. **2**(3): p. 700-705.

34. Caldwell, S.R. and F.M. Raushel, Detoxification of organophosphate pesticides using a nylon based immobilized phosphotriesterase from

Pseudomonas diminuta. Applied Biochemistry and Biotechnology, 1991. **31**(1): p. 59-73.

35. Caldwell, S.R. and F.M. Raushel, Detoxification of organophosphate pesticides using an immobilized phosphotriesterase from *Pseudomonas diminuta*. Biotechnology and Bioengineering, 1991. **37**(2): p. 103-109.

36. Caldwell, S.R. and Raushel, F.M., Detoxification of organophosphate pesticides using a nylon based immobilized phosphotriesterase from *Pseudomonas diminuta*. Biotechnology and Bioengineering, 1991. **31**(1): p. 59-73.

37. Munnecke, D.M., Enzymic detoxification of waste organophosphate pesticides. Journal of Agricultural and Food Chemistry, 1980. **28**(1): p. 105-111.

38. Bhatia, S.K. et al., Biotransformation of lysine into cadaverine using barium alginate-immobilized *Escherichia coli* overexpressing CadA. Bioprocess and Biosystems Engineering, 2015. **38**(12): p. 2315-2322.

39. Seo, H.-M. et al., In situ immobilization of lysine decarboxylase on a biopolymer by fusion with phasin: immobilization of CadA on intracellular PHA. Process Biochemistry, 2016. **51**(10): p. 1413-1419.

40. Steinbüchel, A., Non-biodegradable biopolymers from renewable resources: perspectives and impacts. Current Opinion in Biotechnology, 2005. **16**(6): p. 607-613.

41. Kim, H.J. et al., Optimization of direct lysine decarboxylase biotransformation for cadaverine production with whole-cell biocatalysts at high lysine concentration. J. Microbiol. Biotechnol, 2015. **25**(7): p. 1108-1113.

42. Kim, Y.H. et al., A liquid-based colorimetric assay of lysine decarboxylase and its application to enzymatic assay. J. Microbiol. Biotechnol, 2015. **25**(12): p. 2110-2115.

43. Phan, A., T. Ngo, and H. Lenhoff, Spectrophotometric assay for lysine decarboxylase. Analytical Biochemistry, 1982. **120**(1): p. 193-197.

44. Nishi, K. et al., Method for producing cadaverine dicarboxylate. Journal of

the Taiwan Institute of Chemical Engineers, 2011. **42**(6): p. 607-613.

45. Park, H. et al., Expression, immobilization and enzymatic properties of glutamate decarboxylase fused to a cellulose-binding domain. International Journal of Molecular Sciences, 2012. **13**(1): p. 358-368.

46. Lee, S. et al., Gamma-aminobutyric acid production using immobilized glutamate decarboxylase followed by downstream processing with cation exchange chromatography. International Journal of Molecular Sciences, 2013. **14**(1): p. 1728-1739.

47. Lin, Q., D. Li, and H. Qin, Molecular cloning, expression, and immobilization of glutamate decarboxylase from *Lactobacillus fermentum YS2*. Electronic Journal of Biotechnology, 2017. **27**: p. 8-13.

48. Yao, W. et al., In vitro enzymatic conversion of γ-aminobutyric acid immobilization of glutamate decarboxylase with bacterial cellulose membrane (BCM) and non-linear model establishment. Enzyme and Microbial Technology, 2013. **52**(4-5): p. 258-264.

49. Lee, S.-J., H.-S. Lee, and D.-W. Lee, Production of γ-aminobutyric acid using immobilized glutamate decarboxylase from *Lactobacillus plantarum*. Korean J Microbiol Biotechnol, 2015. **43**: p. 300-5.

50. Gong, J. et al., Determination of γ aminobutyric acid in Chinese rice wines and its evolution during fermentation. Journal of the Institute of Brewing, 2017. **123**(3): p. 417-422.

51. Gomm, A. and E. O'Reilly, Transaminases for chiral amine synthesis. Current Opinion in Chemical Biology, 2018. **43**: p. 106-112.

52. Reis, J.S. et al., Asymmetric reductive amination of boron-containing aryl-ketones using ω-transaminases. Tetrahedron: Asymmetry, 2013. **24**(23): p. 1495-1501.

53. Richter, N. et al., ω-Transaminases for the amination of functionalised cyclic ketones. Organic & Biomolecular Chemistry, 2015. **13**(33): p. 8843-8851.

54. Koszelewski, D. et al., ω-Transaminases for the synthesis of non-racemic α-chiral primary amines. Trends in Biotechnology, 2010. **28**(6): p. 324-332.

55. B.K.Cho, H.Y. Park. et al. Redesigning the substrate specificity of *ω*-Transaminases for the kinetic resolution of aliphatic chiral amines. Biotechol. Bioeng, 2008. **99**: p. 275-284.

56. Mathew, S. and H. Yun, ω-Transaminases for the production of optically pure amines and unnatural amino acids. Acs Catalysis, 2012. **2**(6): p. 993-1001.

57. Molnár, Z. et al., Immobilized whole-Cell transaminase biocatalysts for continuous-flow kinetic resolution of amines. Catalysts, 2019. **9**(5): p. 438.

58. Jia, H. et al., Immobilization of ω-transaminase by magnetic PVA-Fe_3O_4 nanoparticles. Biotechnology Reports, 2016. **10**: p. 49-55.

59. Martin, A.R. et al., Characterization of free and immobilized (S)-aminotransferase for acetophenone production. Applied Microbiology and Biotechnology, 2007. **76**(4): p. 843-851.

60. Yi, S.-S. et al., Covalent immobilization of ω-transaminase from *Vibrio fluvialis JS17* on chitosan beads. Process Biochemistry, 2007. **42**(5): p. 895-898.

61. Mallin, H. et al., Immobilization of two (R) Amine transaminases on an optimized chitosan support for the enzymatic synthesis of optically pure amines. ChemCatChem, 2013. **5**(2): p. 588-593.

62. Päiviö, M. and L.T. Kanerva, Reusable ω-transaminase sol–gel catalyst for the preparation of amine enantiomers. Process Biochemistry, 2013. **48**(10): p. 1488-1494.

63. Truppo, M.D., H. Strotman, and G. Hughes, Development of an immobilized transaminase capable of operating in organic solvent. ChemCatChem, 2012. **4**(8): p. 1071-1074.

초록

다양한 나노fiber를 활용한 효소의 고정화 및 재사용

오소걸

지도교수: 이중헌

조선대학교 화학공학과

효소는 종종 재사용 및 복잡한 회수와 장기간의 작동 안정성 부족으로 인해 방해를 받고 있다. 이러한 단점은 효소의 고정화에 의해 극복 될 수 있다. 이 연구에서, OPH, LDC, GAD 그리고 ω-TA 효소를 foam-PANI, foam-PAMP, foam-PDA 그리고 foam-TA 담체에 고정화하여 높은 안정성을 보였다.

3개월 동안의 연속적인 안정성 측정을 통해서, 고정화 된 효소 foam-PANI-, foam-PAMP-, foam-PDA- 그리고 foam-TA-OPH는 여전히 각각 초기 활성의 87 %, 79 % , 62% 그리고 83 %를 유지하였고, 70시간의 연속적인 반응 후에도 70 %, 72 %, 63 % 그리고 78 %의 전율이 유지되었다.

LDC을 고정화 한 담체의 경우, 3개월 동안의 연속적인 안정성 측정에서, 초기 활성의 0 ~ 6 %만 감소하였고, 80시간동안 연속반응 후에, foam-PANI-, foam-PAMP-, foam-PDA- 그리고 foam-TA-LDC는 여전히 83 %, 80 %, 64 % 및 75 %의 전환율을 유지하였다.

고정화 효소 GAD의 연속적인 3개월 안정성 측정에서, 고정화 효소 foam-PANI-, foam -PAMP-, foam-PDA- 그리고 foam-TA-GAD는 여전히 초기 활성의 89 %, 88 %, 42 % 그리고 81 %을 유지하였다. 연속 생산반응 중에 H^+의 축적으로 효소 활성에 영향을 미치기 때문에 30 시간 후에 생 촉매반응이 감소했다.

이 실험에서 사용된 ω-TA 생성 균주는 야생 균주이며, 효소활성이 낮음에도 불구하고 10회 연속반응 측정에서 고정화 효소 foam-PANI-, foam-PAMP-, foam-PDA- 그리고 foam-TA-(ω-TA)는 42 %, 28 %, 22 %, 및 41 %의 전환율을 꾸준히 유지하였다.

4 가지 재료인 foam-PANI, foam-PAMP, foam-PDA 그리고 foam-TA는 효소 OPH, LDC, GAD 그리고 ω-TA의 고정화 담체로 사용할 수 있음을 확인하였다. 고정화 효소는 생 촉매반응에서 재사용 할 수 있다.